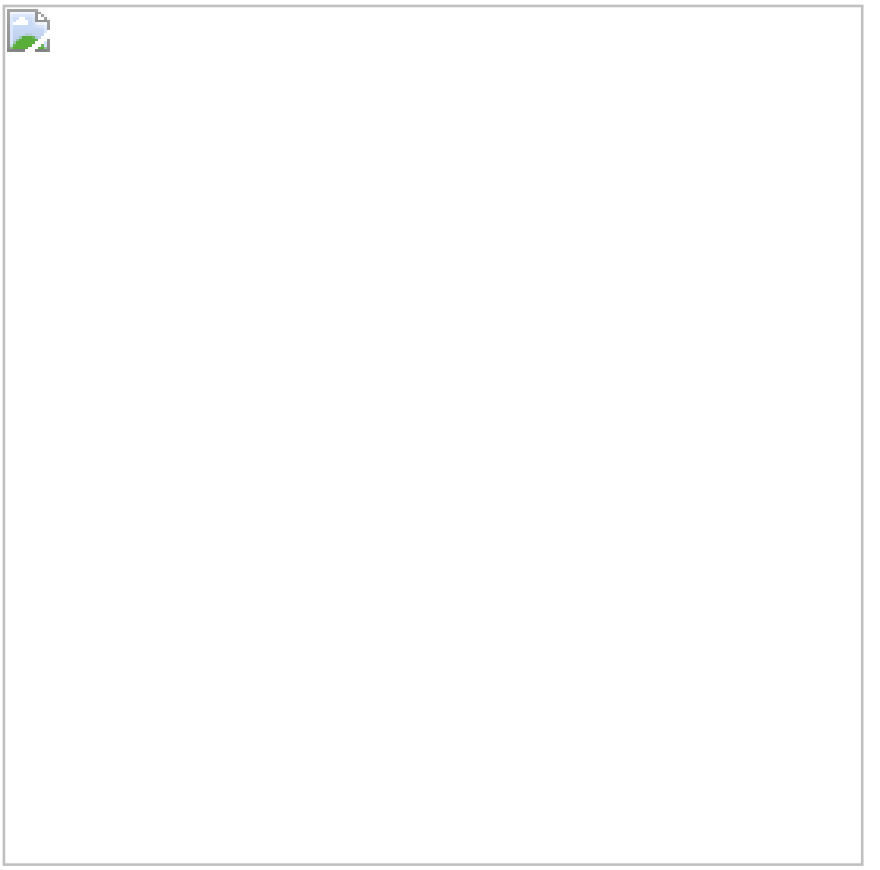

RECONSTRUCTIONS OF HINDLIMB MUSCULATURE IN EXTINCT PRE-THERIAN SYNAPSIDS

Authors: Bishop, P. J., and Pierce, S. E.

Source: Bulletin of the Museum of Comparative Zoology, 163(9) : 417-471

Published By: Museum of Comparative Zoology, Harvard University

URL: https://doi.org/10.3099/MCZ82

Bulletin
of the
Museum of Comparative Zoology

Volume 163, Number 9 11 October 2024

Reconstructions of Hindlimb Musculature in Extinct Pre-therian Synapsids

P. J. Bishop and S. E. Pierce

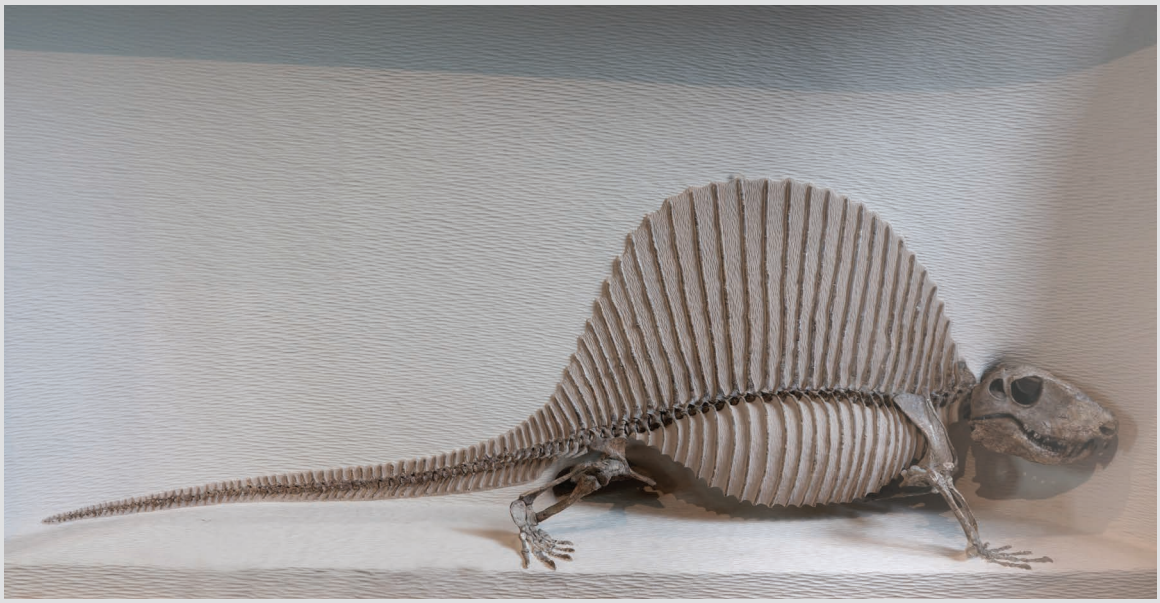

HARVARD UNIVERSITY | CAMBRIDGE, MASSACHUSETTS, U.S.A.

BULLETIN OF THE
Museum of Comparative Zoology

Publications issued or distributed by the
Museum of Comparative Zoology,
Harvard University:

Bulletin 1863–
Breviora 1952–
Memoirs 1865–1938
Johnsonia, Department of Mollusks, 1941–1974
Occasional Papers on Mollusks, 1945–2002

General queries, questions about author guidelines, or permissions for MCZ Publications should be directed to the editorial assistant:

MCZ Publications
Museum of Comparative Zoology
Harvard University
26 Oxford Street
Cambridge, MA 02138

mczpublications@mcz.harvard.edu

EXCHANGES AND REPRINTS

All our publications are available as e-reprints on our website at no charge:
https://mcz.harvard.edu/publicationshome

To join our journal exchange program, please contact the Ernst Mayr Library:
mayrlib@oeb.harvard.edu

This publication has been printed on acid-free permanent paper stock.

RECONSTRUCTIONS OF HINDLIMB MUSCULATURE IN EXTINCT PRE-THERIAN SYNAPSIDS

P. J. BISHOP[1,2] AND S. E. PIERCE[1]

ABSTRACT. Previously, the authors published a framework for phylogenetically informed reconstruction of appendicular musculature in extinct synapsids. In the present study, this framework is employed to rigorously infer the arrangement of muscles in the hindlimb of eight exemplar taxa that capture the evolutionary transformation from basal synapsids to crown therians. Muscle maps detailing origins and insertions are presented for each taxon. These will aid the interpretation of fossil material in the future, especially fragmentary remains of related species, and provide a foundation for functional analysis of the appendicular skeleton and its evolution.

Key words: Fossils, Hindlimb, Mammal, Musculature, Synapsid

INTRODUCTION

The origin and evolution of mammals from nonmammalian synapsid ancestors involved profound anatomical, physiological, and functional reorganization over >100 million years from the earliest synapsids to the first crown therian (Kemp, 1982, 2005, 2016). One system that was greatly transformed during this process was the locomotor apparatus, entailing major changes in posture (from "sprawled" to "erect"), skeletal construction, and muscular topology, differentiation, and coordination, as well as the origin of novel high-speed gaits (e.g., galloping). Although typically not preserved in the fossil record, the arrangement of soft tissues such as musculature has a long history of study in the context of synapsid anatomical and functional evolution (e.g., Watson, 1917; Gregory and Camp, 1918; Romer, 1922; Jenkins, 1971; Kemp, 1980b; Ray and Chinsamy, 2003; Lai et al., 2018). Recently, the authors completed a re-evaluation of appendicular muscle evolution in Synapsida, drawing together a large fossil data set with the anatomy of extant amniotes and integrating this data set into a phylogenetically informed context (Bishop and Pierce, 2024a, 2024b). In addition to offering insight into several higher-level problems in synapsid appendicular evolution, the re-evaluation has provided a new framework for the rigorous interpretation of fossil material across diverse extinct synapsid species.

In the present contribution, this new framework is applied to the reconstruction of hindlimb musculature in exemplar taxa that signpost key evolutionary stages from basal synapsids to therian mammals. Although the pectoral girdle and forelimb underwent more marked skeletal transformation compared to the pelvis and hindlimb, transformation in musculature was more dramatic in the hindlimb (Bishop and Pierce, 2024b). All muscles crossing the hip, knee, and ankle joints are considered here. For some studied taxa, the reconstructions provide revised, more comprehensive updates on prior interpretations (Romer, 1922; Colbert, 1948; Kemp, 1978; DeFauw, 1986), whereas in others, they represent the first attempt at extensive soft tissue inference. The reconstructions ("muscle

[1] Museum of Comparative Zoology and Department of Organismic and Evolutionary Biology, 26 Oxford Street, Harvard University, Cambridge, Massachusetts 02138. Author for correspondence (pbishop@fas.harvard.edu).

[2] Geosciences Program, Queensland Museum, Brisbane, Queensland 4011, Australia.

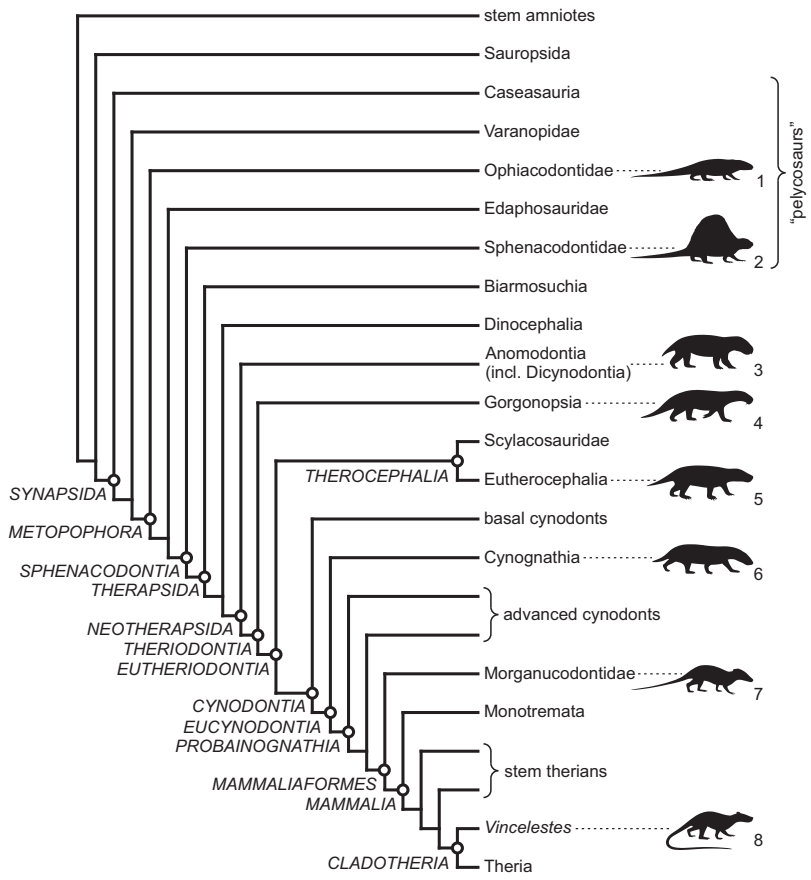

Figure 1. Simplified phylogenetic relationships of the taxa reconstructed here, in the context of the broader interrelationships among Synapsida as a whole. Tree topology follows that used previously (Bishop and Pierce, 2024b; see also Supplementary Information [footnote 1]). Taxon numbers are: 1, *Ophiacodon*; 2, *Dimetrodon*; 3, *Oudenodon*; 4, *Lycaenops*; 5, *Regisaurus*; 6, *Massetognathus*; 7, *Megazostrodon*; 8, *Vincelestes*.

maps") presented here provide an enriched basis for interpreting the anatomy of other fossil species, as well as the requisite anatomical foundation for higher-level functional inferences, such as posture and locomotor behavior (Bishop et al., 2021a).

MATERIALS AND METHODS

Eight extinct taxa (Fig. 1) were reconstructed, chosen on the basis of accessible, well-preserved, and near-complete fossil material, and many have often served as exemplars of their respective clades in prior studies of synapsid anatomy and evolution. *Ophiacodon retroversus* is an ophiacodontid "pelycosaur" (i.e., nontherapsid synapsid) from the early Permian, which retains many traits plesiomorphic for Synapsida as a whole (Romer and Price, 1940; Reisz, 1986). *Dimetrodon milleri* is also a "pelycosaur" from the early Permian, but it represents the derived family Sphenacodontidae, characterized by numerous anatomical modifications shared with therapsids (Romer and Price, 1940; Reisz, 1986; Kemp, 2006). Three "therapsid-grade" taxa are considered here. *Oudenodon bainii* is a bidentalian dicynodont,

a medium-sized representative of a highly diverse lineage of herbivorous taxa that dominated late Permian terrestrial environments and persisted until the end of the Triassic (King, 1990; Botha and Angielczyk, 2007). *Lycaenops ornatus* is a gorgonopsian from the late Permian, often used to illustrate the quintessential therapsid condition (Colbert, 1948; Kemp, 1982). *Regisaurus jacobi* is a baurioid therocephalian from the earliest Triassic, and it has played a key role in prior studies of synapsid locomotor evolution (Kemp, 1978; Blob, 2001). *Massetognathus pascuali* is a cynognathian cynodont from the Middle Triassic in which the postcranial skeletal anatomy is typical of basal eucynodonts in general (Jenkins, 1970). *Megazostrodon* is a morganucodontid mammaliaform from the Early Jurassic, and it is often used as a proxy for the ancestral mammalian condition (Jenkins and Parrington, 1976). Lastly, *Vincelestes neuquenianus* is an Early Cretaceous cladotherian mammal, one of few known from adequate postcranial material (Rougier, 1993; Guignard et al., 2019). Collectively, these taxa capture most of the musculoskeletal changes that occurred on the line to therians (Bishop and Pierce, 2024b).

Reconstruction of musculature drew upon firsthand observations of osteological correlates of muscle attachment in fossil material. Each taxon was scored for 80 character–state complexes described previously (Bishop and Pierce, 2024b), either on its own merit or as part of a higher (generally family-level) taxon; the latter enables the anatomy of other, closely related taxa to inform inferences when direct evidence is absent in the focal taxon itself. When characters were unable to be explicitly scored, character states were reconstructed by maximum parsimony in Mesquite (v.3.6.1; Maddison and Maddison, 2021), assuming a monophyletic Therocephalia, to guide determination of the most plausible origin or insertion. Maximum parsimony is a frequently used approach for phylogenetic inference of soft tissue traits, especially when most operational taxonomic units are suprageneric, although other approaches including maximum likelihood may also be used (Hutchinson, 2001a, 2001b; Hutchinson and Garcia, 2002; Burch, 2014; Molnar et al., 2018, 2020). In the original data set, nontherian cladotherian mammals were not accounted for, so to accommodate *Vincelestes*, a new operational taxonomic unit was created for this taxon and codified as part of the reconstruction process. An updated taxon–character state matrix is provided in Nexus format at https://doi.org/10.3099/MCZ82.[1] To characterize the extent to which inferences for a given muscle are supported by data from fossils and the anatomy of extant amniotes, the credibility scheme of Witmer (1995) was employed (see also Carrano and Hutchinson, 2002). The phylogenetically informed approach employed here does not explicitly facilitate the precise delimitation of muscle origin and insertion boundaries, especially for muscles with fleshy attachments. Reconstructing the extent of muscle attachment areas often relies on the gross osteology observed in the focal species (e.g., shapes and relative sizes of different parts of the bone involved), taking into consideration the (inferred) presence of adjacent musculature and the topological disposition of homologous musculature observed in extant relatives. The illustrations presented here are indicative and should therefore be interpreted with a level of caution (see also Discussion).

Institutional Abbreviations. AMNH, American Museum of Natural History, New York, USA; BP, Evolutionary Studies Institute, University of the Witwatersrand, Johannesburg, South Africa; BSPG, Bayerische Staatssammlung für Paläontologie und Geologie, Munich, Germany; CGS, Council for Geosciences, Pretoria, South Africa; FMNH, Field Museum of Natural History, Chicago, Illinois, USA; GPIT,

[1] Supplementary material referenced in this paper is available online at https://doi.org/10.3099/MCZ82.

Paläontologische Sammlung, Eberhard Karls Universität, Tübingen, Germany; MACN, Museo Argentino de Ciencias Naturales "Bernardino Rivadavia," Buenos Aires, Argentina; MCZ, Museum of Comparative Zoology, Harvard University, Cambridge, Massachusetts, USA; NHMUK, Natural History Museum, London, UK; NMQR, National Museum, Bloemfontein, South Africa; PVL, Instituto Miguel Lillo (Paleovertebrados), Universidad Nacional de Tucumán, Tucumán, Argentina; SAM, Iziko South African Museum, Cape Town, South Africa; TM, Ditsong National Museum of Natural History, Pretoria, South Africa; UMZC, University Museum of Zoology, Cambridge, UK; USNM, National Museum of Natural History, Smithsonian Institution, Washington, D.C., USA.

Muscle Abbreviations. ADD, adductor femoris; ADDB, adductor brevis; ADDL, adductor longus; ADDM, adductor magnus; AMB, ambiens; BICF, biceps femoris; CF, caudofemoralis; EDBh, extensor digitorum brevis (hindlimb); EDLh, extensor digitorum longus (hindlimb); EHL, extensor hallucis longus; FDB, flexor digitorum brevis; FDLh, flexor digitorum longus (hindlimb); FHL, flexor hallucis longus; FMTE, femorotibialis externus; FMTI, femorotibialis internus; FTE, flexor tibialis externus; FTI, flexor tibialis internus; GE, gastrocnemius externus; GEM, gemellus; GI, gastrocnemius internus; GL, gastrocnemius lateralis; GM, gastrocnemius medialis; GMAX, gluteus maximus; GMED, gluteus medius; GMIN, gluteus minimus; GRA, gracilis; IC, interosseus cruris; IF, iliofemoralis; ILFB, iliofibularis; ILPS, iliopsoas; IT, iliotibialis; ISTR, ischiotrochantericus; OBEX, obturator externus; OBIN, obturator internus; PB, peroneus brevis; PECN, pectineus; PIFE, puboischiofemoralis externus; PIFI, puboischiofemoralis internus; PIT, puboischiotibialis; PL, peroneus longus; PLA, plantaris; POP, popliteus; PP, pronator profundus; PUT, pubotibialis; QF, quadratus femoris; RF, rectus femoris; SART, sartorius; SMEM, semimembranosus; STEN, semitendinosus; TA, tibialis anterior; TEN, tenuissimus; TP, tibialis posterior; VL, vastus lateralis; VM, vastus medialis; suffix "a", anterior division; suffix "b", posterior division.

RESULTS

Anatomical terminology for individual bones follows that outlined previously (Bishop and Pierce, 2024b). It is recommended that the reader consult that study for descriptions and interpretations of characters and their states. All reconstructions are illustrated for elements from the right side of the animal.

Ophiacodon retroversus

The reconstruction presented in Figure 2 is based principally on FMNH UC 458, a well-preserved partial skeleton that was extensively featured by Romer and Price (1940). Other specimens in the FMNH and MCZ collections contributed additional information, especially regarding finer-scale nuances of muscle attachments. Inferred origins and insertions are described in Table 1. *Ophiacodon* was codified as part of Ophiacodontidae, and reconstructed states at the node Metopophora (Table S1) were used to clarify remaining uncertainties. Some character states remained ambiguous for this node, and these were resolved for *Ophiacodon* as follows.

Character 12. The iliac blade of ophiacodontids is small, with a restricted area ventral to the transverse line for origin of the IF, supporting reconstruction of a single head in *Ophiacodon* (state 0, level II′ inference in the scheme of Witmer, 1995).

Character 15. Without any positive evidence for a splitting of the muscle mass, the PIFI is conservatively reconstructed as singular here (state 0, level II′ inference). It would be anticipated that, from a functional perspective, two separate heads with highly similar lines of action would not be substantially different from a singular head, assuming

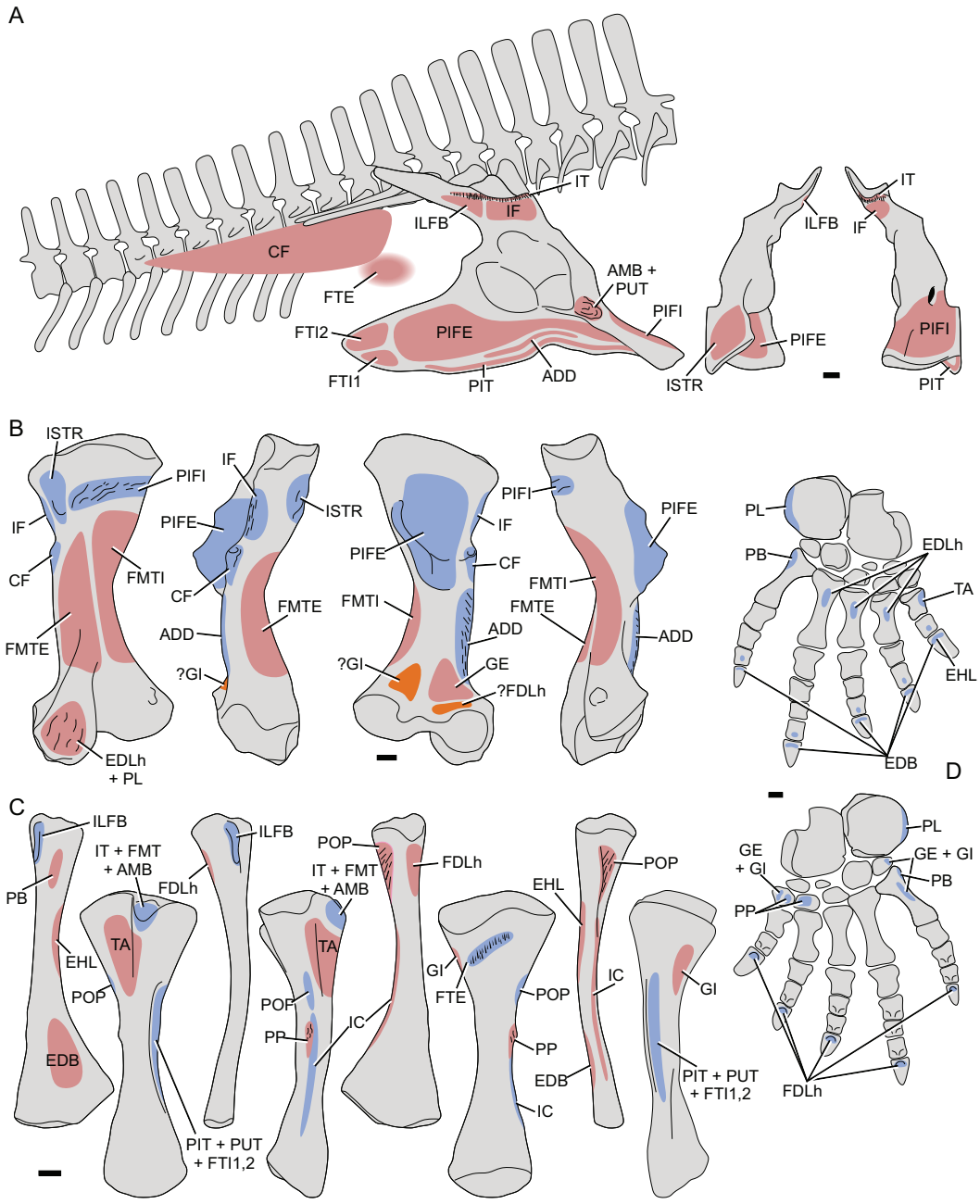

Figure 2. Reconstructed muscle attachments in *Ophiacodon*. A, pelvis and axial skeleton, in lateral, posterior, and anterior views. B, femur in anterior, lateral, posterior, and medial views. C, tibia and fibula in anterior, lateral, posterior, and medial views. D, pes in dorsal (top) and ventral (bottom) views. Red denotes inferred origins, blue denotes inferred insertions, and orange denotes ambiguous attachments (see text). Scale = 10 mm. See Table 1 for muscle abbreviations.

Table 1. Reconstructed origins and insertions in *Ophiacodon retroversus*. LOI, level of inference in the scheme of Witmer (1995).

		Origin		Insertion	
Muscle	Abbreviation	Attachment	LOI	Attachment	LOI
Iliotibialis	IT	Much of dorsolateral iliac blade, along transverse line of scarring; via two heads	II	Tuberosity on anteroproximal end of cnemial crest of tibia, via common "triceps" tendon	I
Ambiens	AMB	Lateral aspect of pubis anteroventral to acetabulum, on or near pubic tubercle	II′	Tuberosity on anteroproximal end of cnemial crest of tibia, via common "triceps" tendon	I
Femorotibialis externus	FMTE	Lateral aspect of much of femoral shaft, distal to IF insertion	I′	Tuberosity on anteroproximal end of cnemial crest of tibia, via common "triceps" tendon	I
Femorotibialis internus	FMTI	Medial aspect of much of femoral shaft, distal to PIFI insertion	I′	Tuberosity on anteroproximal end of cnemial crest of tibia, via common "triceps" tendon	I
Iliofemoralis	IF	Lateral iliac blade immediately dorsal to acetabulum, bounded dorsally by transverse line of scarring	II	Posterolateral aspect of proximal femur, around "posterior ridge" of the posterior fossa (striate scarring), and surrounding bone surface	II
Puboischiofemoralis internus	PIFI	Medial (dorsal) surface of much of puboischiadic plate and symphysis, extending from anterior pubis to anterior ischium; number of divisions uncertain	II′	Anterior to anteromedial proximal femur, proximal and medial to FMTI and IF origins (linear band of fibrous scars)	II
Puboischiofemoralis externus	PIFE	Much of lateral (ventral) surface of puboischiadic plate and symphysis; via two heads	II′	Posterior to posteromedial proximal femur: elongate apex of internal trochanter (anterior head) and intertrochanteric fossa posterior to this (posterior head)	II
Iliofibularis	ILFB	Lateral aspect of postacetabular iliac blade, posterior to IF origin and deep to IT origin	II	Tubercle on anterolateral proximal fibula	II
Flexor tibialis internus	FTI	Posterolateral ischium, with dorsal head originating on or near posterodorsal apex for ischiocaudalis; via at least two heads	II′	Posteromedial tibia, in association with PIT and PUT insertions	II′
Flexor tibialis externus	FTE	Ilioischiadic ligament and fascia covering proximal tail muscles	II′	Posterior proximal tibia (line of striate scarring)	II
Puboischiotibialis	PIT	Much of puboischiadic symphysis and associated puboischiadic ligament	II′	Longitudinal groove on medial tibia, in association with (and superficial to) FTI and PUT	II

TABLE 1. CONTINUED.

		Origin		Insertion	
Muscle	Abbreviation	Attachment	LOI	Attachment	LOI
Pubotibialis	PUT	Anterolateral pubis, on or near pubic tubercle	II′	Posteromedial to medial proximal tibia, in association with PIT and FTE	II
Adductor femoris	ADD	Close to the puboischiadic suture on the ventrolateral puboischiadic plate; may not have involved direct attachment	II′	Posterolateral aspect of femoral shaft distal to fourth trochanter (deep longitudinal crest, often striated)	II
Ischiotrochantericus	ISTR	Posterodorsal (medial) aspect of ischium	II′	Anterolateral proximal femur, immediately lateral to PIFI insertion and proximal to IF insertion (rugose tuberosity)	II
Caudofemoralis	CF	Transverse processes of caudal vertebrae 1–10; via single head	II′	Rugose, knob-like fourth trochanter (with central pit) on posterolateral proximal femur, lateral to distal extent of fossa	II
Gastrocnemius externus	GE	Posterolateral distal femur, proximal to lateral condyle (fibrous scarring)	I	Plantar aponeurosis of the pes, making direct attachment to medial and lateral border of the proximal pes (tarsals) and metatarsal V	II′
Gastrocnemius internus	GI	Posteromedial proximal tibia, distal to FTE insertion	II′	In common with GE	II′
Flexor digitorum longus (hindlimb)	FDLh	Posteromedial aspect of head and proximal shaft of fibula	II′	Plantar aponeurosis of pes, continuing on to insert on flexor tubercles of unguals	II
Flexor digitorum brevis	FDB	Dorsal (deep) surface of plantar aponeurosis and adjacent tarsals and metatarsals	II′	Plantar aspect of proximal phalanges	II′
Extensor digitorum longus (hindlimb)	EDLh	Expanded shelf on anterior aspect of distal femur, immediately proximal to and overhanging lateral condyle (rugose scarring)	II	Dorsal aspect of proximal metatarsals II–IV	II′
Extensor digitorum brevis (hindlimb)	EDBh	Anterior aspect of distal fibula	II′	Dorsal aspect of penultimate phalanges and extensor processes of unguals	I
Extensor hallucis longus	EHL	Anteromedial aspect of midshaft of fibula	II′	Extensor process on dorsal aspect of digit I ungual	II
Tibialis anterior	TA	Anterolateral to anterior aspect of proximal tibia, in lateral fossa and base of cnemial crest	II	Dorsomedial proximal aspect of metatarsal I	II′
Peroneus longus	PL	Expanded shelf on anterior aspect of distal femur, in association with EDLh origin (rugose scarring)	II	Rugose margin of lateral shelf of calcaneum	II

Table 1. Continued.

Muscle	Abbreviation	Origin		Insertion	
		Attachment	LOI	Attachment	LOI
Peroneus brevis	PB	Anterolateral proximal fibula	II′	Lateral aspect of base of metatarsal V	II′
Pronator profundus	PP	Lateral aspect of tibial shaft, along localized line of fibrous scarring and tubercles trending distally (distinct from more proximal scar for POP, and more faint longitudinal ridge for IC)	II	Plantar aspect of medial distal tarsals	II′
Popliteus	POP	Proximomedial fibular shaft (coarse, striate scarring)	II	Posterolateral proximal tibia	II
Interosseus cruris	IC	Medial distal fibular shaft, distal to POP origin	II′	Ridge on lateral tibial shaft, adjacent to PP origin	II′

that their combined mass and force-generating capacity were the same as that of the singular head.

Character 16. The plesiomorphic, anteroposteriorly expansive puboischiadic plate, and minimal preacetabular extension of the iliac blade, strongly supports reconstructing the PIFI origin in the primitive state in all "pelycosaurs" (state 0, level II′ inference).

Character 18. There is no positive evidence for a splitting of the muscle mass in "pelycosaurs." and conservatively a single head would be reconstructed. However, the inferred origin (character 19) occupies an extensive area, rendering it more likely that some level of anteroposterior subdivision existed, at least in function if not actual anatomy (state 1, level II′ inference).

Character 19. Much like character 16, the plesiomorphic morphology of the puboischiadic plate suggests the PIFE existed in the primitive state in all "pelycosaurs" (state 0, level II′ inference).

Character 27. The FTI2 is synapomorphic for Amniota (character 23), and so it can be inferred to have existed in *Ophiacodon*. As hypothesized by Bishop and Pierce (2024b), the persistence of a fibular tubercle suggests that the switch from ILFB-dominated (TEN-dominated) to FTI2-dominated (BICF-dominated) attachment on the fibula probably occurred crownward of Mammaliaformes. An insertion on the tibia is therefore reconstructed here (state 1, level II′ inference).

Character 28. The presence of the FTE is most parsimoniously inferred as a synapomorphy of Amniota (or a more inclusive clade), and only a single head is conservatively assumed here for the FTE (state 1, level II′ inference).

Character 29. The FTE was present in "pelycosaurs" (see previous character), but no osteological correlate of its origin is present (i.e., not states 0 or 3). The locus of its attachment would have been somewhere between the posterior ilium and dorsal ischium, and it is tentatively reconstructed in the middle of this area, spanning between the two bones via soft tissues (state 1, level II′ inference). A dorsoventrally shallow posterior ilium in *Ophiacodon* further argues against any attachment to this bone. In functional terms, the exact dorsal position of origin would only be expected to have a potentially important effect on the capacity for hip elevation (limb abduction) and depression.

Character 30. The posterior proximal tibia of large, well-preserved *Ophiacodon* specimens bears a characteristic linear region of rugose scarring (Bishop and Pierce, 2024b). The scars are always directed proximally, suggesting that they denote insertion of either one or more of the long flexors (excluding the PIT), or the POP. A feature arguing against the latter is the inclination of the linear region, such that the scars are not well suited for receiving a muscle spanning from the fibula laterally. It is not possible to identify which long flexor(s) inserted here, but the FTE usually is one of the more laterally inserting of the muscles in extant species, and as the dorsalmost one in origin, it is topographically "easiest" to reconstruct as inserting here in extinct forms such as *Ophiacodon*. A FTE insertion is tentatively inferred here (level II inference).

Character 31. The FTE can be confidently reconstructed as present in *Ophiacodon*, and in light of the lack of any positive osteological evidence, the conservative assumption is that a secondary attachment to the GL was absent (state 2, level II′ inference).

Character 34. "Pelycosaurs" are inferred to have retained the plesiomorphic configuration of the PIFI mass (characters 15 and 16), which in turn implies that the PUT also existed in its primitive, single-bellied condition (state 0, level II′ inference).

Character 35. Following the same logic as for the preceding character, a singular insertion is reconstructed for the PUT (state 0, level II′ inference).

Character 37. As the ADD is unambiguously reconstructed as possessing a single head (character 36), this obviates the possibility of a crocodylian-like origin. However, it is not possible to discern between the remaining potential states in the absence of osteological evidence; whether or not it gained direct osteological attachment to the pubis and/or ischium is uncertain. A conservative, middle-of-the-road approach is taken here, and the origin is reconstructed as close to the puboischiadic suture on the ventrolateral puboischiadic plate, which is topographically intermediate between states 1 and 3 (level II′ inference). Whether a direct osteological attachment was present or not would have negligible effect in functional terms.

Character 38. Phylogenetic optimization recovers state 1 as unambiguous for Metopophora; however, *Ophiacodon retroversus* itself codes as state 2 here.

Character 43. The tail of "pelycosaurs" is extensive, although the region typically associated with the CF origin in extant long-tailed sauropsids (long head) is notably shorter in "pelycosaurs" (Bishop and Pierce, 2024b); for example, transverse processes are completely absent by the 11th caudal vertebra in MCZ VPRA-1366 *Ophiacodon uniformis*. The locus of origin in tetrapods is primitively an osseous attachment somewhere in the ventrolateral quadrant of the proximal tail, but exactly where direct attachment occurred, and whether this included the posterior ilium, is uncertain. The origin is tentatively inferred to be restricted to just the proximal caudal vertebrae in *Ophiacodon* (state 0, level II′ inference).

Character 46. The gastrocnemii are ubiquitous among amniotes, and so the GE can be confidently inferred as present in "pelycosaurs." Absence of a calcaneal tuber, fabellae, or parafibula in "pelycosaurs," coupled with the plesiomorphic "flattened" nature of the tarsals, suggests that the GE most likely existed in the primitive, single-headed condition in *Ophiacodon* (state 1, level II′ inference).

Character 48. As per character 46, a distinct PLA is considered absent in *Ophiacodon* (state 0, level II′ inference).

Character 50. The (at least partial) involvement of the posterior to medial proximal tibia in the GI origin is widespread across amniotes. The posteromedial proximal tibia area is here conservatively reconstructed as the primary locus of the origin

for the GI in *Ophiacodon* (state 1, level II′ inference), but an attachment to the distal femur is not implausible.

Character 51. The GE can be inferred as present in *Ophiacodon*, but the absence of a calcaneal tuber implies the plesiomorphic, aponeurotic form of insertion (state 1, level II′ inference).

Character 52. As per character 46, a distinct PLA is considered absent in *Ophiacodon* (state 0, level II′ inference).

Character 54. As per character 51, a common aponeurotic insertion with the GE is reconstructed (state 1, level II′ inference).

Character 55. The locus of the FDLh origin in amniotes is generally centered around the posterior proximal fibula, and this area is conservatively inferred to be the primary attachment for the FDLh in *Ophiacodon* (state ~3, level II′ inference; parafibula is unknown in "pelycosaurs"). However, it cannot be ruled out that the origin extended more proximally to include the distal femur.

Character 62. In the absence of any positive osteological evidence, the plesiomorphic state is reconstructed for *Ophiacodon* here (state 0, level II′ inference).

Character 64. Plesiomorphically, the general locus of origin for the EDBh is the ankle joint, but extant mammals exhibit an origin near the proximal fibula; the origin presumably underwent proximal migration on the line to mammals. The EDBh in *Ophiacodon* is conservatively inferred to originate from the anterior aspect of the distal fibula (state 2, level II′ inference), spatially midway between the mammalian and nonmammalian conditions.

Character 66. The EHL is ubiquitous among amniotes and can be confidently inferred as present in "pelycosaurs." Its locus of origin is centered around the anterior fibula, and in the absence of any positive evidence, a middle-of-the-road approach is taken, reconstructing the muscle's origin in *Ophiacodon* at the fibular midshaft (state 2, level II′ inference).

Character 69. An insertion of the TA distal to the ankle is ubiquitous among amniotes, with the general locus of attachment located at metatarsal I. A more plesiomorphic insertion on the anteromedial proximal aspect of metatarsal I is reconstructed here (state 1, level II′ inference), which is consonant with the more "reptilian" construction of the pes in "pelycosaurs," namely, a primitive tarsal configuration, broad and flat proximal tarsals, and strong asymmetry in digit lengths.

Character 72. Two peroneal heads can be confidently reconstructed (character 70), permitting reconstruction of the PB as originating from the anterolateral proximal fibula in *Ophiacodon* (state 3, level II′ inference).

Character 74. Two peroneal heads can be confidently reconstructed (character 70), with the PB inserting in a mammal-like fashion somewhere along pedal ray V. An insertion on metatarsal V is inferred here (state 4, level II′ inference).

Character 75. Strictly speaking, unambiguous osteological evidence is wanting for this character in ophiacodontids, and phylogenetic inference results in state 0 being reconstructed here. However, the lateral tibial shaft possesses a distinctive line of fibrous or rugose scarring, with the scars "trending" distally, and these scars in some specimens are clearly separate from the rugose scarring proximally inferred as the attachment of the POP. A similar condition is observed in some other "pelycosaurs" as well (Bishop and Pierce, 2024b, fig. 29). This may denote a tibial attachment for the PP (state 1, level II inference), or alternatively for the IC.

Character 76. The plesiomorphic condition of the "pelycosaur" pes suggests that a more mammal-like insertion of the PP is unlikely; in any case, the locus of insertion was probably centered on the plantar aspect of the medial pes. A primary attachment to the medial distal tarsals is inferred here (state 2, level II′ inference).

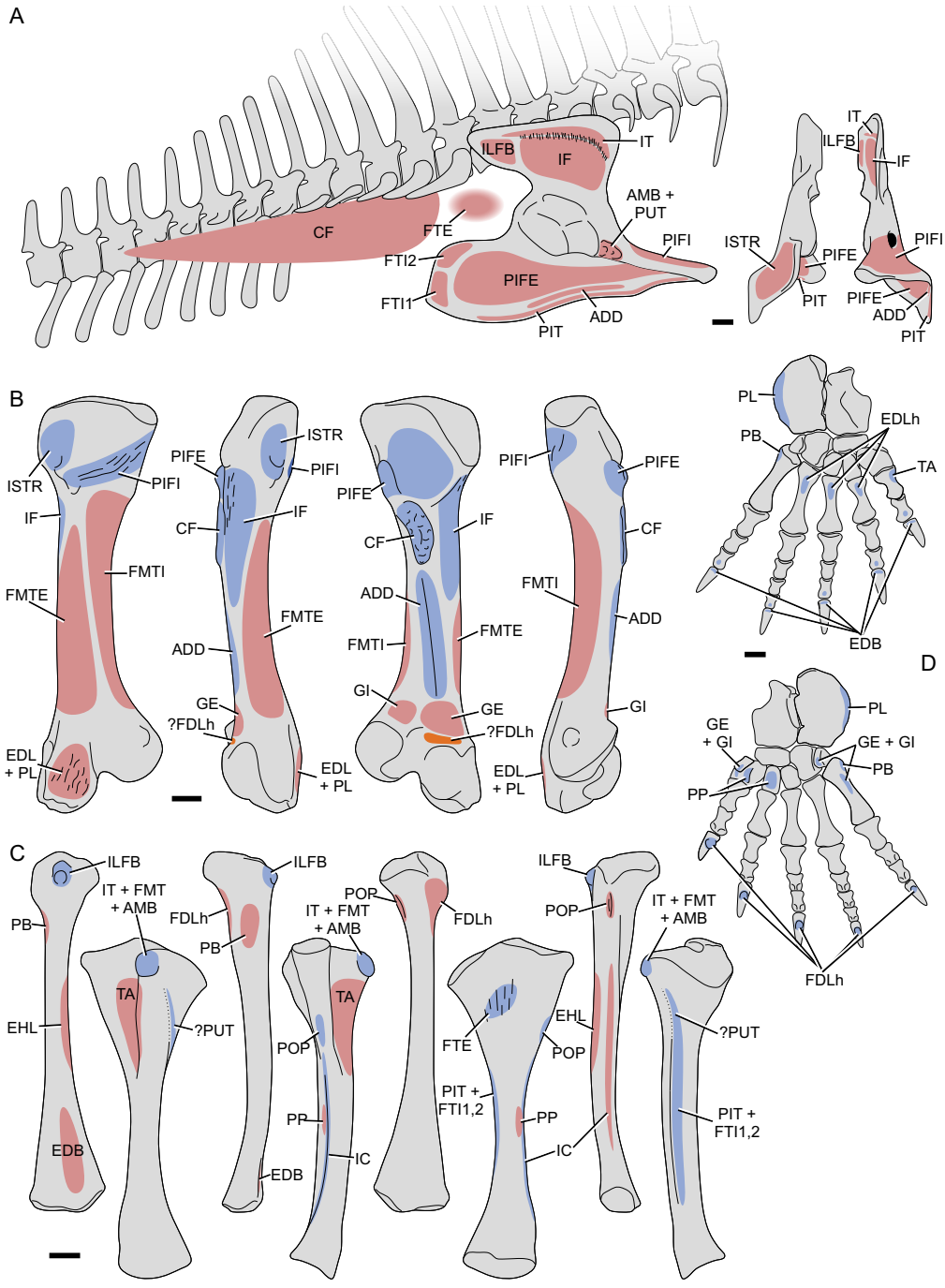

Figure 3. Reconstructed muscle attachments in *Dimetrodon.* A, pelvis and axial skeleton, in lateral, posterior, and anterior views. B, femur in anterior, lateral, posterior, and medial views. C, tibia and fibula in anterior, lateral, posterior, and medial views. D, pes in dorsal (top) and ventral (bottom) views. Red denotes inferred origins, blue denotes inferred insertions, and orange denotes ambiguous attachments (see text). Scale = 10 mm. See Table 2 for muscle abbreviations.

Dimetrodon milleri

The reconstruction presented in Figure 3 is based principally on the holotype, MCZ VPRA-1365, a near-complete individual (Romer and Price, 1940), although other specimens of various *Dimetrodon* species in the MCZ, FMNH, and AMNH collections furnished additional information. Inferred origins and insertions are described in Table 2. *Dimetrodon* was codified as part of a paraphyletic "Sphenacodontia" (see Bishop and Pierce, 2024b), and reconstructed states at the node Sphenacodontia *sensu stricto* (Table S2) were used to clarify remaining uncertainties. Some character states remained ambiguous for this node, and these were resolved for *Dimetrodon* as follows.

Character 12. The iliac blade of sphenacodontians remains of modest size, conservatively suggesting that only a single head was still present in *Dimetrodon* (state 0, level II′ inference). However, it is notably expanded relative to more basal "pelycosaurs," suggesting that the IF at least had a larger origin, if not physically subdivided (character 13; see Bishop and Pierce, 2024b).

Character 15. Without any positive evidence for a splitting of the muscle mass, the PIFI is conservatively reconstructed as singular here (state 0, level II′ inference).

Character 16. The plesiomorphic, anteroposteriorly expansive puboischiadic plate, and minimal preacetabular extension of the iliac blade, strongly supports reconstructing the PIFI origin in the primitive state in all "pelycosaurs" (state 0, level II′ inference).

Character 18. There is no positive evidence for a splitting of the PIFE mass in "pelycosaurs," and conservatively a single head would be reconstructed. However, as explained above for *Ophiacodon*, it is probable that some level of anteroposterior subdivision existed (state 1, level II′ inference).

Character 19. Much like character 16, the plesiomorphic morphology of the puboischiadic plate suggests the PIFE existed in the primitive state in all "pelycosaurs" (state 0, level II′ inference).

Character 27. Following the same logic as outlined above for *Ophiacodon*, an insertion on the tibia is reconstructed for *Dimetrodon* (state 1, level II′ inference).

Character 28. The presence of the FTE is most parsimoniously inferred as a synapomorphy of Amniota (or a more inclusive clade), and only a single head is conservatively inferred for the FTE (state 1, level II′ inference).

Character 29. The FTE was present in "pelycosaurs" (see previous character), but no osteological correlate of its origin is present (i.e., not states 0 or 3). The locus of its attachment would have been somewhere between the posterior ilium and dorsal ischium, and it is tentatively reconstructed in the middle of this area, spanning between the two bones via soft tissues (state 1, level II′ inference).

Character 30. The posterior proximal tibia of large, well-preserved *Dimetrodon* specimens (especially of *limbatus* and *grandis* species) bears a broad, diffuse region of notably more rugose bone texture, sometimes quite similar to that which is characteristic of large *Ophiacodon* specimens (Bishop and Pierce, 2024b). Following the same logic for *Ophiacodon*, a FTE insertion is inferred here (level II inference).

Character 31. The FTE can be confidently reconstructed as present in *Dimetrodon*, and in light of the lack of any positive osteological evidence, the conservative assumption is that a secondary attachment to the GL was absent (state 2, level II′ inference).

Character 34. "Pelycosaurs" are inferred to have retained the plesiomorphic configuration of the PIFI mass (characters 15 and 16), which in turn implies that the PUT also existed in its primitive, single-bellied condition (state 0, level II′ inference).

Character 35. Following the same logic as for the preceding character, a singular

TABLE 2. RECONSTRUCTED ORIGINS AND INSERTIONS IN *DIMETRODON MILLERI*. LOI, LEVEL OF INFERENCE IN THE SCHEME OF WITMER (1995).

		Origin		Insertion	
Muscle	Abbreviation	Attachment	LOI	Attachment	LOI
Iliotibialis	IT	Much of dorsal lateral iliac blade, bounded ventrally by transverse line of scarring; via two heads	II	Tuberosity on anteroproximal end of cnemial crest of tibia, via common "triceps" tendon	I
Ambiens	AMB	Lateral aspect of pubis anteroventral to acetabulum, on or near pubic tubercle	II′	Tuberosity on anteroproximal end of cnemial crest of tibia, via common "triceps" tendon	I
Femorotibialis externus	FMTE	Lateral aspect of much of femoral shaft, anterior (medial) to IF insertion	I′	Tuberosity on anteroproximal end of cnemial crest of tibia, via common "triceps" tendon	I
Femorotibialis internus	FMTI	Medial aspect of much of femoral shaft, distal and lateral to PIFI insertion	I′	Tuberosity on anteroproximal end of cnemial crest of tibia, via common "triceps" tendon	I
Iliofemoralis	IF	Lateral iliac blade immediately dorsal (and anterior) to acetabulum, bounded dorsally by transverse line of scarring	II	Posterolateral aspect of proximal femur, around "posterior ridge" of the posterior fossa (striate scarring), and surrounding bone surface	II
Puboischiofemoralis internus	PIFI	Medial (dorsal) surface of much of puboischiadic plate and symphysis, extending from anterior pubis to anterior ischium; number of divisions uncertain	II′	Anterior to anteromedial proximal femur, proximal and medial to FMTI and IF origins (linear band of fibrous scars)	II
Puboischiofemoralis externus	PIFE	Much of lateral (ventral) surface of puboischiadic plate and symphysis; via two heads	II′	Posterior to posteromedial proximal femur: apex of internal trochanter (anterior head) and fossa posterior to this (posterior head)	II
Iliofibularis	ILFB	Lateral aspect of postacetabular iliac blade, posterior to IF origin and deep to IT origin	II	Tubercle on anterolateral proximal fibula	II
Flexor tibialis internus	FTI	Posterolateral ischium, with dorsal head originating on or near posterodorsal apex for ischiocaudalis; via at least two heads	II′	Anteromedial to medial tibia, in association with PIT and PUT insertions	II′
Flexor tibialis externus	FTE	Ilioischiadic ligament and fascia covering proximal tail muscles	II′	Posterior proximal tibia (striate scarring)	II
Puboischiotibialis	PIT	Much of puboischiadic symphysis and associated puboischiadic ligament	II′	Longitudinal groove on medial tibia (extending proximally toward cnemial crest apex via line of rugose bone or tubercles), in association with (and superficial to) FTI and PUT	II

Table 2. Continued.

Muscle	Abbreviation	Origin		Insertion	
		Attachment	LOI	Attachment	LOI
Pubotibialis	PUT	Anterolateral pubis, on or near pubic tubercle	II′	Anteromedial to medial proximal tibia, in association with PIT and FTE	II
Adductor femoris	ADD	Close to the puboischiadic suture on the ventrolateral puboischiadic plate; may not have involved direct attachment	II′	Posterolateral aspect of femoral shaft distal to internal and fourth trochanters (faint longitudinal ridge of rugosities)	II
Ischiotrochantericus	ISTR	Posterodorsal (medial) aspect of ischium, in shallow depression facing dorsomedially	II	Anterolateral proximal femur, immediately lateral to PIFI insertion and proximal to IF insertion (rugose tuberosity)	II
Caudofemoralis	CF	Transverse processes of caudal vertebrae 1–10; via single head	II′	Rugose fourth trochanter on posterior proximal femur, immediately distal to fossa	II
Gastrocnemius externus	GE	Posterolateral distal femur, proximal to lateral condyle (fibrous scarring)	I	Plantar aponeurosis of the pes, making direct attachment to medial and lateral border of the proximal pes (tarsals) and metatarsal V	II′
Gastrocnemius internus	GI	Posteromedial distal femur, proximal to medial condyle (fibrous scarring)	II	In common with GE	II′
Flexor digitorum longus (hindlimb)	FDLh	Posteromedial aspect of head and proximal shaft of fibula	II′	Plantar aponeurosis of pes, continuing on to insert on flexor tubercles of unguals	II
Flexor digitorum brevis	FDB	Dorsal (deep) surface of plantar aponeurosis and adjacent tarsals and metatarsals	II′	Plantar aspect of proximal phalanges	II′
Extensor digitorum longus (hindlimb)	EDLh	Expanded shelf on anterior aspect of distal femur, immediately proximal to and overhanging lateral condyle (rugose scarring)	II	Dorsal aspect of proximal metatarsals II–IV	II′
Extensor digitorum brevis (hindlimb)	EDBh	Anterior aspect of distal fibula	II′	Dorsal aspect of penultimate phalanges and extensor processes of unguals	I
Extensor hallucis longus	EHL	Anteromedial aspect of midshaft of fibula	II′	Extensor process on dorsal aspect of digit I ungual	II
Tibialis anterior	TA	Anterolateral to anterior aspect of proximal tibia, in lateral fossa and base of cnemial crest	II	Dorsomedial proximal aspect of metatarsal I	II′
Peroneus longus	PL	Expanded shelf on anterior aspect of distal femur, in association with EDLh origin (rugose scarring)	II	Rugose margin of lateral shelf of calcaneum	II

TABLE 2. CONTINUED.

		Origin		Insertion	
Muscle	Abbreviation	Attachment	LOI	Attachment	LOI
Peroneus brevis	PB	Anterolateral proximal fibula	II′	Lateral aspect of base of metatarsal V	II′
Pronator profundus	PP	Lateral aspect of tibial shaft, along line of fibrous scarring trending distally (distinct from more proximal scar for POP)	II	Plantar aspect of medial distal tarsals	II′
Popliteus	POP	Proximomedial fibular shaft (tuberosity)	II	Posterolateral proximal tibia (scarring)	II
Interosseus cruris	IC	Medial distal fibular shaft, distal to POP origin	II′	Lateral tibial shaft, adjacent to PP origin	II′

insertion is reconstructed for the PUT in *Dimetrodon* (state 0, level II′ inference).

Character 37. Following the same argument as outlined above for *Ophiacodon*, the ADD origin is inferred as close to the puboischiadic suture on the ventrolateral puboischiadic plate, which is intermediate between states 1 and 3 (level II′ inference).

Character 43. The tail of "pelycosaurs" is extensive, although the region typically associated with the CF origin in extant long-tailed sauropsids is notably shorter in "pelycosaurs"; for example, transverse processes are completely absent by the 11th caudal vertebra in MCZ VPRA-1365. The locus of origin in tetrapods is primitively an osseous attachment somewhere in the ventrolateral quadrant of the proximal tail, but exactly where direct attachment occurred, and whether this included the posterior ilium, is uncertain. The origin is tentatively inferred to have been restricted to just the proximal caudal vertebrae in *Dimetrodon* (state 0, level II′ inference).

Character 46. The gastrocnemii are ubiquitous among amniotes, and so the GE can be confidently inferred as present in "pelycosaurs." Absence of a calcaneal tuber, fabellae, or parafibula in "pelycosaurs," coupled with the plesiomorphic plate-like geometry of the tarsals, suggests that the GE most likely existed in the primitive, single-headed condition in *Dimetrodon* (state 1, level II′ inference).

Character 48. As per character 46, a distinct PLA was not present in *Dimetrodon* (state 0, level II′ inference).

Character 51. The GE can be inferred as present in *Dimetrodon*, but the absence of a calcaneal tuber implies the plesiomorphic, aponeurotic form of insertion (state 1, level II′ inference).

Character 52. As per character 46, a distinct PLA was not present in *Dimetrodon* (state 0, level II′ inference).

Character 54. As per character 51, a common aponeurotic insertion with the GE is inferred here (state 1, level II′ inference).

Character 55. The locus of the FDLh origin in amniotes is generally centered around the posterior proximal fibula, and this area is conservatively reconstructed as the primary attachment for the FDLh in *Dimetrodon* (state ~3, level II′ inference; parafibula is unknown in "pelycosaurs"). As in *Ophiacodon*, it cannot be ruled out that the origin extended more proximally to include the distal femur.

Character 62. In the absence of any positive osteological evidence, the plesiomorphic state is assumed here for *Dimetrodon* (state 0, level II′ inference).

Character 64. Following the same argument as outlined above for *Ophiacodon*,

the EDBh origin is inferred as centered on the anterior aspect of the distal fibula (state 2, level II′ inference).

Character 66. The EHL is ubiquitous among amniotes and can be confidently inferred as present in "pelycosaurs." Its locus of origin is centered around the anterior fibula, and in the absence of any positive evidence, a middle-of-the-road approach is taken to reconstruct its origin in *Dimetrodon* at the fibular midshaft (state 2, level II′ inference).

Character 69. An insertion of the TA distal to the ankle is ubiquitous among amniotes, with the general locus of attachment located at metatarsal I. A more plesiomorphic insertion on the anteromedial proximal aspect of metatarsal I is inferred here (state 1, level II′ inference).

Character 72. Following the same argument as outlined above for *Ophiacodon*, the PB likely originated from the anterolateral proximal fibula in *Dimetrodon* (state 3, level II′ inference).

Character 74. Following the same argument as outlined above for *Ophiacodon*, the insertion of the PB is inferred to be on metatarsal V (state 4, level II′ inference).

Character 75. Following the same argument as outlined above for *Ophiacodon*, a tibial attachment for the PP is inferred here for *Dimetrodon* (state 1, level II inference).

Character 76. Following the same argument as outlined above for *Ophiacodon*, a primary attachment to the medial distal tarsals is inferred here (state 2, level II′ inference).

Oudenodon bainii

The reconstruction presented in Figure 4 is based principally on NHMUK PV R.4067, a very well preserved and mostly complete skeleton (Watson, 1917, 1960). Material in the BP, GPIT, and SAM collections provided additional details for parts of the pelvis that were missing. The pes of NHMUK PV R.4067 is not preserved, and as such, the pedal anatomy was based on other material, especially that of NMQR 479 *Dicynodontoides recurvidens*, an excellently preserved and complete specimen missing only the tip of the ungual from digit III (King, 1985). Inferred origins and insertions are described in Table 3. *Oudenodon* was codified as part of Anomodontia, and reconstructed states at the node Neotherapsida (Table S3) were used to clarify remaining uncertainties. Some character states remained ambiguous for this node, and these were resolved for *Oudenodon* as follows.

Character 12. The apomorphic anterior expansion of the iliac blade in therapsids suggests enlargement and probable differentiation of the primitive iliofemoralis mass, and so two heads are conservatively reconstructed here (state 1, level II′ inference).

Character 13. This is reconstructed unambiguously as state 1 for Neotherapsida, but within dicynodonts (including *Oudenodon*), the preacetabular blade further expands anteriorly, coding as state 2.

Character 15. Without any positive evidence for a splitting of the muscle mass, the PIFI mass is conservatively reconstructed as singular here (state 0, level II′ inference).

Character 16. The reduction of the pubis in dicynodonts such as *Oudenodon* suggests a more dorsal location for the origin of the PIFI on the pubis (Bishop and Pierce, 2024b), but likely not extending onto the ilium (state 2, level II inference).

Character 18. There is no positive evidence for a splitting of the PIFE muscle mass in dicynodonts, and conservatively a single head would be reconstructed. However, in a similar fashion to the "pelycosaurs," as the inferred origin (character 19) covers a broad area, this suggests some degree of anteroposterior subdivision, presaging the mammalian OBEX (anterior) and QF (posterior).

Character 19. Character optimization is ambiguous for Neotherapsida, but the greatly reduced and posteriorly swept pubis

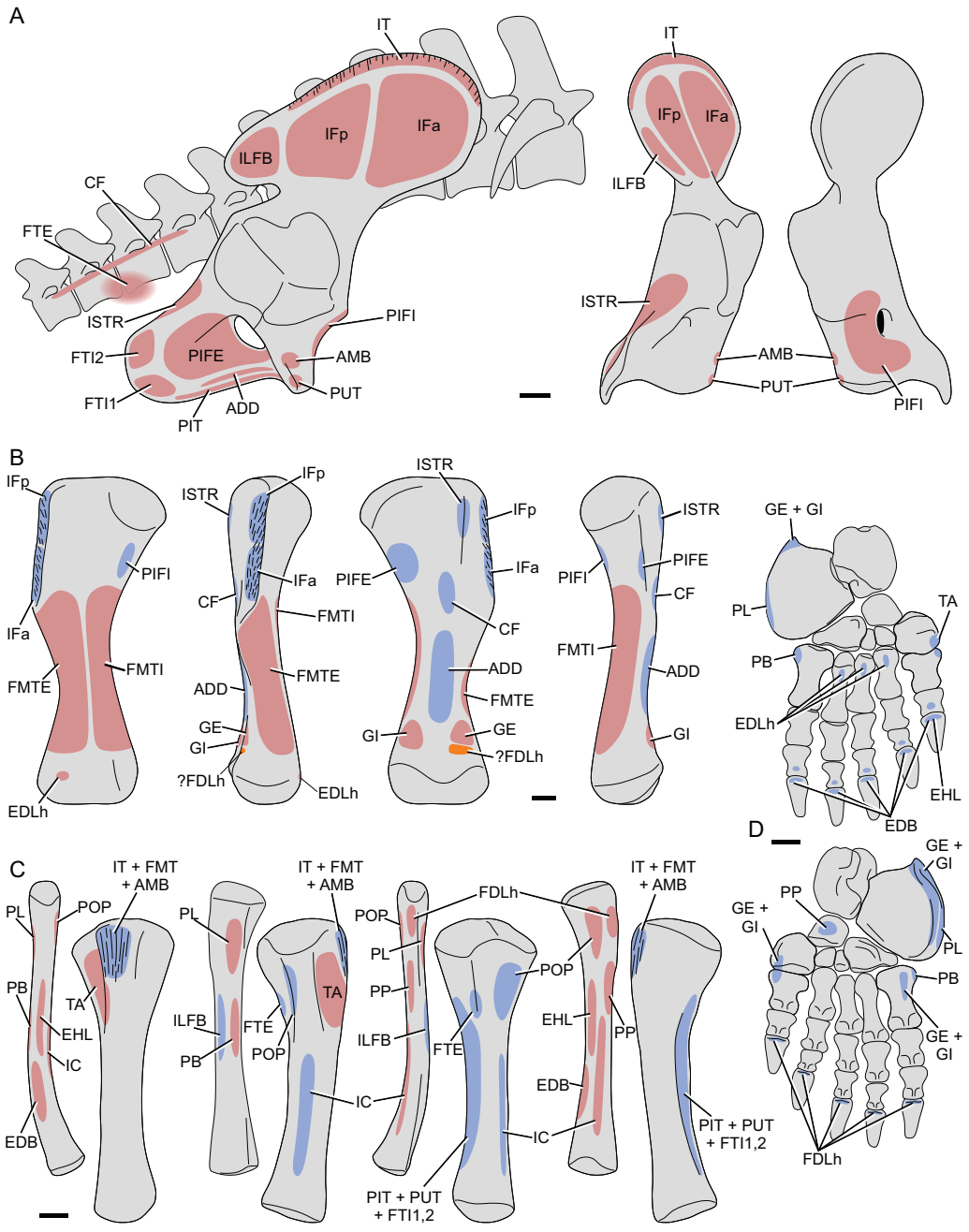

Figure 4. Reconstructed muscle attachments in *Oudenodon.* A, pelvis and axial skeleton, in lateral, posterior, and anterior views. B, femur in anterior, lateral, posterior, and medial views. C, tibia and fibula in anterior, lateral, posterior, and medial views. D, pes in dorsal (top) and ventral (bottom) views; based on *Dicynodontoides*. Red denotes inferred origins, blue denotes inferred insertions, and orange denotes ambiguous attachments (see text). Scale = 10 mm. See Table 3 for muscle abbreviations.

Table 3. Reconstructed origins and insertions in *Oudenodon bainii*. LOI, level of inference in the scheme of Witmer (1995).

		Origin		Insertion	
Muscle	Abbreviation	Attachment	LOI	Attachment	LOI
Iliotibialis	IT	Much of dorsal and anterodorsal rim of iliac blade (thickened or rugose margin); via two heads	II	Scarring on anteroproximal end of cnemial crest of tibia, via common "triceps" tendon	I
Ambiens	AMB	Lateral aspect of pubis anteroventral to acetabulum, on or near pubic tubercle	II′	Scarring on anteroproximal end of cnemial crest of tibia, via common "triceps" tendon	I
Femorotibialis externus	FMTE	Lateral aspect of much of femoral shaft, distal to IF insertions	I′	Scarring on anteroproximal end of cnemial crest of tibia, via common "triceps" tendon	I
Femorotibialis internus	FMTI	Medial aspect of much of femoral shaft, distal and lateral to PIFI insertion	I′	Scarring on anteroproximal end of cnemial crest of tibia, via common "triceps" tendon	I
Iliofemoralis	IF	Much of lateral surface of preacetabular iliac blade, dorsal and anterior to acetabulum; via two heads	II′	Anterolateral aspect of greater trochanter on lateral proximal femur	II
Puboischiofemoralis internus	PIFI	Dorsomedial surface of pubis; number of divisions uncertain	II′	Anteromedial aspect of proximal femur	II′
Puboischiofemoralis externus	PIFE	Much of lateral surface of pubis and ischium surrounding obturator foramen; via two heads	II′	Posteromedial aspect of proximal femur, on vestigial internal trochanter (scarred bump)	II
Iliofibularis	ILFB	Lateral aspect of postacetabular iliac blade, posterior to IF origin and deep to IT origin	II	Tubercle/scarring on lateral fibula, around midshaft	II
Flexor tibialis internus	FTI	Posterolateral ischium, with dorsal head (FTI2) originating on posterodorsal apex; via at least two heads	II′	Posteromedial tibia, in association with PIT and FTI insertions	II′
Flexor tibialis externus	FTE	Ilioischiadic ligament and fascia covering proximal tail	II′	Posteromedial tibia, in association with PIT and FTI insertions	II′
Puboischiotibialis	PIT	Ventral pubis and ischium along puboischiadic symphysis	II′	Longitudinal groove on medial tibia, in association with (and superficial to) FTI, FTE, and PUT	II
Pubotibialis	PUT	Anterolateral pubis, on or near pubic tubercle	II′	Anteromedial to medial proximal tibia, in association with PIT and FTE	II′
Adductor femoris	ADD	Close to the puboischiadic suture on the ventrolateral puboischiadic plate; may not have involved direct attachment	II′	Posterior aspect of distal femoral shaft	II′

TABLE 3. CONTINUED.

Muscle	Abbreviation	Origin		Insertion	
		Attachment	LOI	Attachment	LOI
Ischiotrochantericus	ISTR	Dorsolateral ischium (shallow, longitudinal depression facing dorsolaterally), plus medial surface of ischium	II	Posterior aspect of greater trochanter (scarring)	II
Caudofemoralis	CF	Transverse processes of posterior sacral vertebrae and proximalmost caudal vertebrae; via single head	II′	Posterior aspect of femoral shaft, distal to PIFE insertion	II′
Gastrocnemius externus	GE	Posterolateral distal femur, proximal to lateral condyle (scarring)	I	Ventral aspect of calcaneum and metatarsals	II′
Gastrocnemius internus	GI	Posteromedial distal femur, proximal to medial condyle (scarring)	II	In common with GE	II′
Flexor digitorum longus (hindlimb)	FDLh	Posteromedial aspect of head and proximal shaft of fibula	II′	Tendon that runs to insert on flexor tubercles of unguals	II
Flexor digitorum brevis	FDB	Dorsal (deep) surface of plantar fascia and adjacent tarsals and metatarsals	II′	Plantar aspect of proximal phalanges	II′
Extensor digitorum longus (hindlimb)	EDLh	Anterior aspect of distal femur proximal to lateral condyle	II′	Dorsal aspect of proximal metatarsals II–IV	II′
Extensor digitorum brevis (hindlimb)	EDBh	Anterior aspect of distal fibula	II′	Dorsal aspect of penultimate phalanges and extensor processes of unguals	I
Extensor hallucis longus	EHL	Anteromedial aspect of midshaft of fibula	II′	Extensor process on dorsal aspect of digit I ungual	II
Tibialis anterior	TA	Anterolateral aspect of proximal tibia, in lateral fossa of cnemial crest	II	Dorsomedial proximal aspect of entocuneiform or metatarsal I	II′
Peroneus longus	PL	Lateral proximal fibula	II′	Distolateral shelf ("peroneal shelf") of calcaneum	II
Peroneus brevis	PB	Anterolateral proximal fibula, anterior to PL origin	II′	Lateral aspect of base of metatarsal V	II′
Pronator profundus	PP	Posteromedial aspect of proximal fibular shaft, distal to FDLh origin	II′	Plantar aspect of navicular	II′
Popliteus	POP	Medial aspect of fibular head and proximal shaft	II	Posterolateral proximal tibia	II
Interosseus cruris	IC	Medial aspect of distal fibular shaft	II′	Lateral aspect of distal tibial shaft	II′

and enlarged obturator foramen of most dicynodonts (including *Oudenodon*) support state 2 (level II′ inference).

Character 27. The FTI2 is synapomorphic for Amniota (character 23), and so can be inferred to have existed in *Oudenodon*. As discussed above for the "pelycosaurs," an insertion on the tibia can be reconstructed (state 1, level II′ inference).

Character 28. The presence of the FTE is most parsimoniously inferred as a synapomorphy of Amniota (or a more inclusive clade), and only a single head is conservatively assumed for the FTE here (state 1, level II′ inference).

Character 29. The FTE was present in dicynodonts (see previous character), but no osteological correlate of its origin is present (i.e., not states 0 or 3). The locus of its attachment would have been somewhere between the posterior ilium and dorsal ischium, although the reduction of the postacetabular ilium in dicynodonts suggests that the FTE probably did not attach there. The muscle's origin is tentatively reconstructed in the middle, spanning between the two bones via soft tissues (state 1, level II′ inference). In functional terms, the exact dorsal position of origin would only be expected to have a potentially important effect on hip elevation–depression capacity. Derived kannemeyeriiform dicynodonts usually possess an ischiadic tuberosity much like that of cynodonts, which may signal in those animals a reconfiguration of the crural long flexor origins (Bishop and Pierce, 2024b).

Character 31. The FTE can be confidently reconstructed as present in *Oudenodon*. Following the same logic as outlined for the "pelycosaurs," a secondary attachment to the GL was probably absent (state 2, level II′ inference).

Character 34. Although dicynodonts are inferred to have a dorsally shifted PIFI origin (character 16 above), this is not homologous to the similar shift inferred to have taken place within cynodonts (Bishop and Pierce, 2024b; see also below), and so it cannot be *a priori* expected to have been accompanied by changes to the PUT. In the absence of evidence to the contrary, the plesiomorphic condition is conservatively reconstructed, with a single origin on or near the pubic tubercle (state 0, level II′ inference).

Character 35. Following the same logic as for the preceding character, a plesiomorphic, singular insertion is reconstructed in *Oudenodon* (state 0, level II′ inference).

Character 37. As the ADD is unambiguously reconstructed as possessing a single head (character 36), this obviates the possibility of a crocodylian-like origin. However, it is not possible to discern between the remaining potential states in the absence of osteological evidence. It cannot be determined whether attachment to the pubis and/or ischium was direct or indirect (via a ligament or aponeurosis). A similar approach to the "pelycosaurs" is taken here, with an origin inferred as close to the puboischiadic junction on the ventrolateral puboischiadic plate, which is intermediate between states 1 and 3 (level II′ inference).

Character 43. The greatly reduced tail of dicynodonts suggests a more mammalian type of origin for the CF. *Oudenodon* is tentatively reconstructed with the monotremes' condition, in which a small osseous contact remains (state 2, level II′ inference).

Character 46. The gastrocnemii are ubiquitous among amniotes, and so the GE can be confidently inferred as present in dicynodonts. Even in well-preserved, articulated skeletons of dicynodonts, there is no evidence for ossified fabellae, or a parafibula, which might signal subdivision (although *Dicynodontoides* possesses an incipient calcaneal tuber; King, 1985). Without any positive evidence for a splitting of the muscle mass, the GE is conservatively reconstructed as singular here (state 1, level II′ inference).

Characters 48 and 52. As per character 46, a distinct PLA was not present in *Oudenodon* (state 0, level II′ inference).

Character 51. Due to the presence of a calcaneal tuber in the biarmosuchian *Hippposaurus*, maximum parsimony reconstructs the presence of such a feature as plesiomorphic for Neotherapsida. This is obviously highly improbable, given the suite of non-eutheriodont taxa that lack any such process. Only *Dicynodontoides* possesses a weak, incipient tuber, hinting at some change to the nature of insertion. A middle-of-the-road state is inferred for *Oudenodon*, between states 1 and 3, with the GE forming an abbreviated plantar aponeurosis that only attaches to the ventral aspect of the calcaneum and metatarsals.

Character 55. The locus of the FDLh origin in amniotes is generally centered around the posterior proximal fibula; this area is conservatively reconstructed as the primary attachment for the FDLh in *Oudenodon* (state ~3, level II′ inference; parafibula is unknown in non-cynodont therapsids).

Character 61. Osteological evidence is wanting for this character, but the locus of origin of the EDLh can confidently be inferred to have been somewhere around the anterolateral aspect of the knee. Two out of the three available states involve the lateral femoral condyle, and although the distal femur lacks the lateral shelf of "pelycosaurs," the proximal fibula remains robustly developed in therapsids, lacking a spatulate profile or parafibular development (i.e., a more plesiomorphic configuration). The attachment in *Oudenodon* is tentatively assumed to be centered on the distal femur (approximating state 1, level II′ inference).

Character 62. In the absence of any positive osteological evidence, the plesiomorphic state is reconstructed for *Oudenodon* here (state 0, level II′ inference).

Character 64. Following the same logic as outlined for *Ophiacodon*, the EDBh in *Oudenodon* is inferred to originate from the anterior aspect of the distal fibula (state 2, level II′ inference). Its proximal path is inferred as along the anterior face of the fibula, rather than between fibula and tibia, to reflect the muscle approaching a more "mammalian" position.

Character 66. The EHL is ubiquitous among amniotes and can be confidently inferred as present in dicynodonts. Its locus of origin is centered around the anterior fibula, and in the absence of any positive evidence, a middle-of-the-road approach is taken, with the muscle's origin in *Oudenodon* reconstructed at the fibular midshaft (state 2, level II′ inference).

Character 69. An insertion of the TA distal to the ankle is ubiquitous among amniotes, with the general locus of attachment located at metatarsal I. Although the tarsal arrangement is generally difficult to assess in most anomodonts due to poor preservation or lower levels of ossification, at least some anomodonts have the same arrangement as observed in extant mammals (Brinkman, 1981; King, 1985). This is tentatively taken to indicate that *Oudenodon* possessed a more mammal-like attachment of the TA, on the entocuneiform in addition to metatarsal I (state 3, level II′ inference).

Character 71. The PL can unambiguously be inferred to have originated from around the lateral knee region, but the specific location cannot be discerned in therapsids. Two of the three available states involve the lateral proximal fibula, and while the fibula retains a (plesiomorphically) robust proximal construction, an origin from this region is tentatively inferred (state 3, level II′ inference).

Character 72. Two peroneal heads can be confidently reconstructed (character 70), permitting reconstruction of the PB as originating from the anterolateral proximal fibula in *Oudenodon* (state 3, level II′ inference).

Character 74. Two peroneal heads can be confidently reconstructed (character 70), with the PB inserting in a mammal-like

fashion somewhere along pedal ray V. An insertion on metatarsal V is inferred here (state 4, level II′ inference).

Character 76. Given that at least some anomodonts possess a mammalian tarsal arrangement, this suggests that *Oudenodon* may have possessed a more mammal-like attachment of the PP on the plantar aspect of the proximal tarsals (state 3, level II′ inference).

Lycaenops ornatus

The reconstruction presented in Figure 5 is based principally on AMNH FARB 2240, the holotype and a generally well-preserved, near-complete skeleton (Colbert, 1948). All elements are contained within the mount on public display, which could not be disassembled for detailed study. Thus, in some cases, the inferences for *Lycaenops* were more heavily dependent on observations of other gorgonopsian material in BP, SAM, GPIT, UMZC, TM, BSPG, CGS, USNM, and NMQR collections, assuming gross similarity (without evidence to the contrary). Inferred origins and insertions are described in Table 4. *Lycaenops* was codified as part of Gorgonopsia, and reconstructed states at the node Theriodontia (Table S4) were used to clarify remaining uncertainties. Some character states remained ambiguous for this node, and these were resolved for *Lycaenops* as follows.

Character 12. The apomorphic anterior expansion of the therapsid iliac blade suggests enlargement and probable differentiation of the primitive iliofemoralis mass, and so two heads are conservatively reconstructed here (state 1, level II′ inference).

Character 15. Without any positive evidence for a splitting of the muscle mass, the PIFI is conservatively reconstructed as singular here (state 0, level II′ inference).

Character 16. Although gorgonopsians, including *Lycaenops*, typically have an abbreviated pubis ventrally with a constricted ischiadic peduncle, it is nonetheless still anteroposteriorly extensive. The plesiomorphic state is hence reconstructed here (state 0, level II′ inference).

Character 18. There is no positive evidence for a splitting of the muscle mass in gorgonopsians, and conservatively a single head would be reconstructed. However, in a similar fashion to the "pelycosaurs," as the inferred origin (character 19) covers a broad area, this suggests some degree of anteroposterior subdivision, presaging the mammalian OBEX (anterior) and QF (posterior).

Character 19. Theriodontia is ambiguous for this character (0, 1, 2), but gorgonopsians including *Lycaenops* possess an abbreviated pubis and are hence are able to be coded as state 1 (level II′ inference; see Bishop and Pierce, 2024b).

Character 20. In *Lycaenops* specifically, the internal trochanter is greatly reduced, although a broad patch of scarring in the same place as the trochanter (present in other gorgonopsians) is present, indicating the insertion of the PIFE (state 3, level II inference).

Character 27. The FTI2 is synapomorphic for Amniota (character 23), and so it can be inferred to have existed in *Lycaenops*. As outlined for *Oudenodon* above, an insertion on the tibia is also reconstructed here (state 1, level II′ inference).

Character 28. The presence of the FTE is most parsimoniously inferred as a synapomorphy of Amniota (or a more inclusive clade), and only a single head is conservatively assumed here (state 1, level II′ inference).

Character 29. The FTE was present in gorgonopsians (see previous character), but no osteological correlate of its origin is present (i.e., not states 0 or 3). The locus of its attachment would have been somewhere between the posterior ilium and dorsal ischium. In a similar fashion to *Oudenodon*, the origin is inferred to be located in the middle, spanning between the two bones via soft tissues (state 1, level II′ inference).

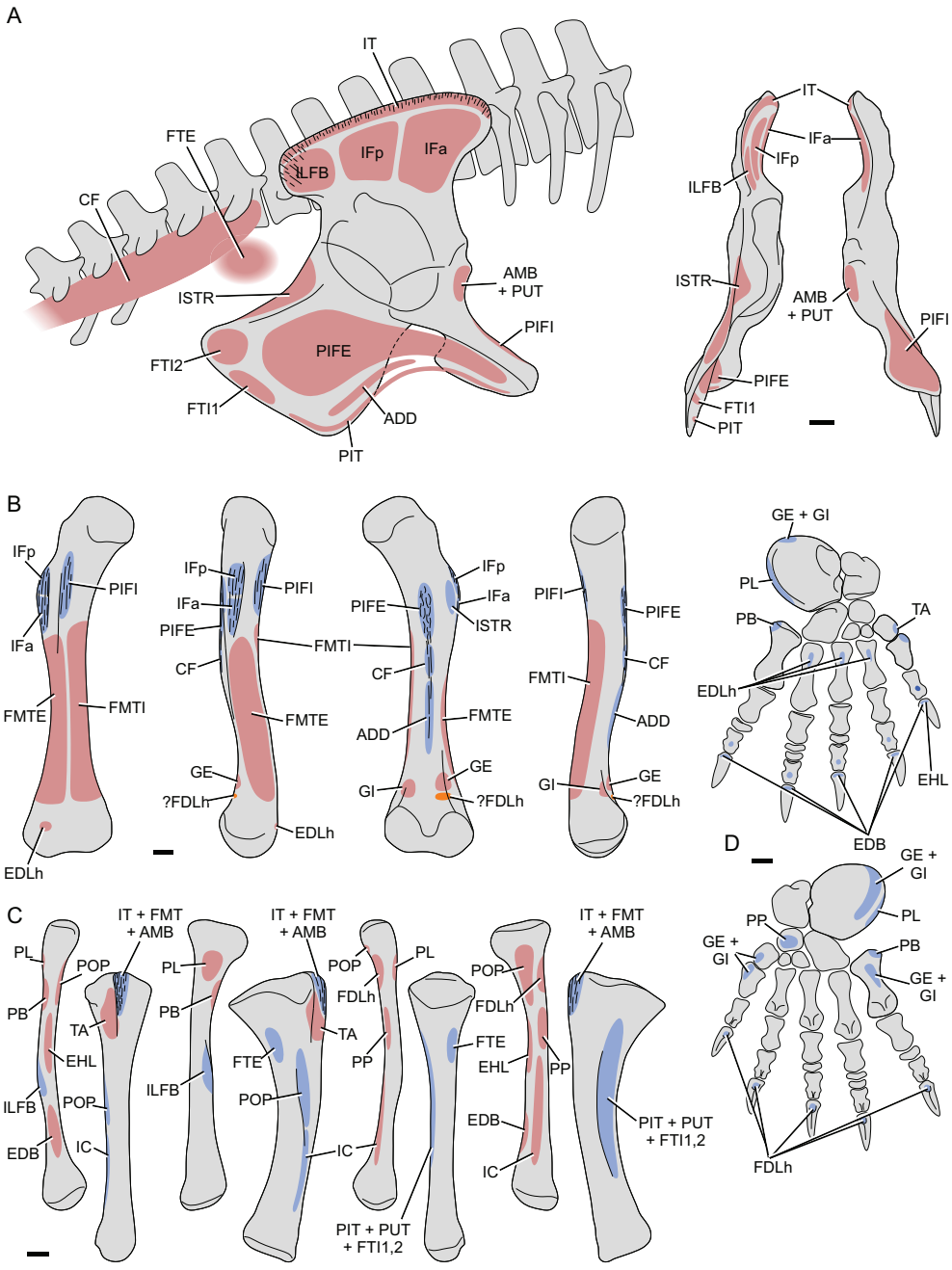

Figure 5. Reconstructed muscle attachments in *Lycaenops*. A, pelvis and axial skeleton, in lateral, posterior, and anterior views. B, femur in anterior, lateral, posterior, and medial views. C, tibia and fibula in anterior, lateral, posterior, and medial views. D, pes in dorsal (top) and ventral (bottom) views. Red denotes inferred origins, blue denotes inferred insertions, and orange denotes ambiguous attachments (see text). Scale = 10 mm. See Table 4 for muscle abbreviations.

Table 4. Reconstructed origins and insertions in *Lycaenops ornatus*. LOI, level of inference in the scheme of Witmer (1995).

		Origin		Insertion	
Muscle	Abbreviation	Attachment	LOI	Attachment	LOI
Iliotibialis	IT	Much of dorsal and anterodorsal rim of iliac blade (thickened or rugose margin); via two heads	II	Scarring on anteroproximal end of cnemial crest of tibia, via common "triceps" tendon	I
Ambiens	AMB	Lateral aspect of pubis anteroventral to acetabulum, on or near pubic tubercle	II′	Scarring on anteroproximal end of cnemial crest of tibia, via common "triceps" tendon	I
Femorotibialis externus	FMTE	Lateral aspect of much of femoral shaft, distal to IF insertions	I′	Scarring on anteroproximal end of cnemial crest of tibia, via common "triceps" tendon	I
Femorotibialis internus	FMTI	Medial aspect of much of femoral shaft, distal and lateral to PIFI insertion	I′	Scarring on anteroproximal end of cnemial crest of tibia, via common "triceps" tendon	I
Iliofemoralis	IF	Much of lateral surface of preacetabular iliac blade, dorsal and anterior to acetabulum; via two heads	II′	Anterolateral aspect of greater trochanter on lateral proximal femur	II
Puboischiofemoralis internus	PIFI	Medial (dorsal) surface of much of puboischiadic plate and symphysis, extending from anterior pubis to anterior ischium; number of divisions uncertain	II′	Anteromedial aspect of proximal femur (longitudinal area of scarring)	II
Puboischiofemoralis externus	PIFE	Much of lateral surface of pubis and (especially) ischium surrounding obturator foramen; via two heads	II′	Posteromedial aspect of proximal femur, on internal trochanter (scarring)	II
Iliofibularis	ILFB	Lateral aspect of postacetabular iliac blade, posterior to IF origin and deep to IT origin (scarring)	II	Tubercle/scarring on lateral fibula, distal to midshaft	II
Flexor tibialis internus	FTI	Posterolateral ischium, with dorsal head (FTI2) originating on posterodorsal apex; via at least two heads	II′	Posteromedial tibia, in association with PIT and FTI insertions	II′
Flexor tibialis externus	FTE	Ilioischiadic ligament and fascia covering proximal tail	II′	Posteromedial proximal tibia (scarred bump)	II
Puboischiotibialis	PIT	Ventral pubis and ischium along puboischiadic symphysis	II′	Longitudinal groove on medial tibia, in association with (and superficial to) FTI and PUT	II
Pubotibialis	PUT	Anterolateral pubis, on or near pubic tubercle	II′	Anteromedial to medial proximal tibia, in association with PIT and FTI	II′

TABLE 4. CONTINUED.

Muscle	Abbreviation	Origin		Insertion	
		Attachment	LOI	Attachment	LOI
Adductor femoris	ADD	Anterior margin of ventrolateral ischium; may not have involved direct attachment	II′	Posterior aspect of distal femoral shaft (longitudinal line of scarring)	II
Ischiotrochantericus	ISTR	Dorsolateral ischium (shallow, longitudinal depression facing dorsolaterally), plus medial surface of ischium	II	Posterior aspect of greater trochanter	II′
Caudofemoralis	CF	Transverse processes of caudal vertebrae 1–8 (approximately); via single head	II′	Posterior aspect of femoral shaft, distal to PIFE insertion	II′
Gastrocnemius externus	GE	Posterolateral distal femur, proximal to lateral condyle (scarring)	I	Ventral aspect of calcaneum and metatarsals	II′
Gastrocnemius internus	GI	Posteromedial distal femur, proximal to medial condyle	II′	In common with GE	II′
Flexor digitorum longus (hindlimb)	FDLh	Posteromedial aspect of head and proximal shaft of fibula	II′	Tendon that runs to insert on flexor tubercles of unguals	II
Flexor digitorum brevis	FDB	Dorsal (deep) surface of plantar fascia and adjacent tarsals and metatarsals	II′	Plantar aspect of proximal phalanges	II′
Extensor digitorum longus (hindlimb)	EDLh	Anterior aspect of distal femur proximal to lateral condyle	II′	Dorsal aspect of proximal metatarsals II–IV	II′
Extensor digitorum brevis (hindlimb)	EDBh	Anterior aspect of distal fibula	II′	Dorsal aspect of penultimate phalanges and extensor processes of unguals	I
Extensor hallucis longus	EHL	Anteromedial aspect of midshaft of fibula	II′	Extensor process on dorsal aspect of digit I ungual	II
Tibialis anterior	TA	Anterolateral aspect of proximal tibia, in lateral fossa of cnemial crest	II	Dorsomedial proximal aspect of entocuneiform or metatarsal I	II′
Peroneus longus	PL	Lateral proximal fibula	II′	Distolateral shelf ("peroneal shelf") of calcaneum	II
Peroneus brevis	PB	Anterolateral proximal fibula, anterior to PL origin	II′	Lateral aspect of base of metatarsal V	II′
Pronator profundus	PP	Posteromedial aspect of proximal fibular shaft, distal to FDLh origin	II′	Plantar aspect of navicular	II′
Popliteus	POP	Medial aspect of fibular head and proximal shaft	II	Posterolateral proximal tibia	II
Interosseus cruris	IC	Medial aspect of distal fibular shaft	II′	Lateral aspect of distal tibial shaft	II′

Character 30. The posterior proximal tibia of some well-preserved gorgonopsian specimens bears a discrete region of rugose scarring (Bishop and Pierce, 2024b). This is located in a comparable location to scarring often observed in "pelycosaurs" (including *Ophiacodon* and *Dimetrodon*), as well as some other therapsid groups, and it probably denotes the insertion of a long flexor muscle. It is not possible to identify which long flexor(s) inserted here, but following the same logic as outlined for the other taxa above, a FTE insertion is inferred here in *Lycaenops* (level II inference).

Character 31. The FTE can be confidently reconstructed as present in *Lycaenops*. Following the same logic as outlined above for other taxa, a secondary attachment to the GL was probably absent (state 2, level II′ inference).

Character 34. The PIFI in gorgonopsians is inferred to have manifested in the plesiomorphic state (character 16), and so there is no evidence to suggest that modifications to the PUT had occurred by this point in synapsid evolution. The plesiomorphic condition is reconstructed for *Lycaenops*, having a single origin on or near the pubic tubercle (state 0, level II′ inference).

Character 35. Following the same logic as for the preceding character, a plesiomorphic, singular insertion is inferred in *Lycaenops* (state 0, level II′ inference).

Character 37. Following the same logic as outlined above for *Oudenodon*, the ADD origin is inferred as near the anterior margin of the ventrolateral ischium, which is intermediate between states 1 and 3 (level II′ inference).

Character 38. Gorgonopsians can variably exhibit states 0 (level II′ inference) and 1 (level II inference); *Lycaenops* in particular has a smooth posterior femoral shaft (state 0).

Character 43. The tail of gorgonopsians is not well known, and a complete series of caudal vertebrae have yet to be described (although the tail of the basal *Viatkogorgon* appears to be almost complete, comprising at least 20 vertebrae; Tatarinov, 2004). Available specimens indicate that the tail, whilst relatively short in relation to the body, was still solidly constructed, with well-developed transverse processes continuing up to at least caudal vertebra 8 (Colbert, 1948; von Huene, 1950; Tatarinov, 2004; personal observation of USNM material). This suggests that the CF probably retained a more plesiomorphic origin from the caudal vertebrae only, not yet having shifted its locus anteriorly toward the sacrals (state 0, level II′ inference).

Character 46. The gastrocnemii are ubiquitous among amniotes, and so the GE can be confidently inferred as present in gorgonopsians. Even in well-preserved, articulated skeletons of gorgonopsians, there is no evidence for ossified fabellae, or a parafibula, which might signal subdivision (although several specimens possess an incipient calcaneal heel). Without any positive evidence for a splitting of the muscle mass, the GE is conservatively reconstructed as singular here (state 1, level II′ inference).

Characters 48 and 52. As per character 46, a distinct PLA was not present in *Lycaenops* (state 0, level II′ inference).

Character 51. As noted above for *Oudenodon*, maximum parsimony reconstructs the presence of a calcaneal tuber as plesiomorphic for Theriodontia, despite most non-eutheriodont taxa lacking any such process. Some gorgonopsian specimens possess a weak, incipient tuber or heel, hinting at some change to the nature of insertion (Bishop and Pierce, 2024b). A middle-of-the-road state is inferred for *Lycaenops*, between states 1 and 3, with the GE forming an abbreviated plantar aponeurosis that only attaches to the ventral aspect of the calcaneum and metatarsals.

Character 55. The locus of the FDLh origin in amniotes is generally centered around the posterior proximal fibula; this area is conservatively reconstructed as the primary attachment for the FDLh in *Lycaenops* (state ~3, level II′ inference; parafibula is unknown in non-cynodont therapsids).

Character 61. Following the same logic as outlined above for *Oudenodon*, the attachment in *Lycaenops* is assumed to be centered on the femur (approximating state 1, level II′ inference).

Character 62. In the absence of any positive osteological evidence, the plesiomorphic state is reconstructed here for *Lycaenops* (state 0, level II′ inference).

Character 64. Following the same logic as outlined above for *Oudenodon*, the EDBh in *Lycaenops* is reconstructed as originating from the anterior aspect of the distal fibula (state 2, level II′ inference).

Character 66. Following the same logic as outlined above for *Oudenodon*, the origin of the EHL in *Lycaenops* is reconstructed at the fibular midshaft (state 2, level II′ inference).

Character 69. An insertion of the TA distal to the ankle is ubiquitous among amniotes, with the general locus of attachment located at metatarsal I. Gorgonopsians already had achieved the tarsal arrangement observed in extant mammals (Boonstra, 1934; Broili and Schröder, 1935; Colbert, 1948; Sidor, 2022; Bendel et al., 2023), suggesting that *Lycaenops* likely possessed a more mammal-like attachment of the TA, on the entocuneiform in addition to metatarsal I (state 3, level II′ inference).

Character 71. Following the same logic as outlined above for *Oudenodon*, the PL in *Lycaenops* is inferred to have originated from around the proximal fibula (state 3, level II′ inference).

Character 72. Following the same logic as outlined above for *Oudenodon*, the PB likely originated from the anterolateral proximal fibula in *Lycaenops* (state 3, level II′ inference).

Character 74. Following the same logic as outlined above for *Oudenodon*, the PB of *Lycaenops* likely inserted on metatarsal V (state 4, level II′ inference).

Character 76. Given that gorgonopsians possess a mammalian tarsal arrangement, this suggests that *Lycaenops* may have possessed a more mammal-like attachment of the PP on the plantar aspect of the proximal tarsals (state 3, level II′ inference).

Regisaurus jacobi

The reconstruction presented in Figure 6 is based principally on the holotype, BP/1/5394, which insofar as the hindlimb is concerned is substantially complete and well preserved, lacking the pubis, ischium, and distal pes (Kemp, 1978). The anatomy of the pubis and ischium in the reconstruction is based on that in other well-preserved eutherocephalian specimens, including UMZC T.837 *Scaloposaurus constrictus* (Kemp, 1986), SAM-PK-K8798 *Choerosaurus dejageri* (Haughton, 1929), and BP/1/3973 *Olivierosuchus parringtoni* (Fourie and Rubidge, 2007). The anatomy of the distal pes is likewise informed from specimens including UMZC T.837, BP/1/4021 *Scaloposaurus* sp., SAM-PK-K10704 *Ictidosuchoides* cf. *longiceps*, and AMNH FARB 5622 *Bauria cynops* (Schaeffer, 1941). Inferred origins and insertions are described in Table 5. *Regisaurus* was codified as part of Eutherocephalia, and reconstructed states at the node Therocephalia (Table S5) were used to clarify remaining uncertainties. Use of an alternative tree topology, wherein Therocephalia is paraphyletic with respect to Cynodontia (Bishop and Pierce, 2024a, 2024b; see also Pusch et al., 2024), did not change the results. Some character states remained ambiguous for this node, and these were resolved for *Regisaurus* as follows.

Character 2. Although the state is unambiguous for *Regisaurus*, the exact location on the ilium is ambiguous, given the uncertainty in precisely when the migration of the ITa to RF took place (Bishop and Pierce, 2024b). Therocephalian ilia are characterized by two anteriorly directed processes on the anterior-to-dorsal margin, the lower one of which is especially pronounced in *Regisaurus*. It remains uncertain if the development of these processes was related to appendicular

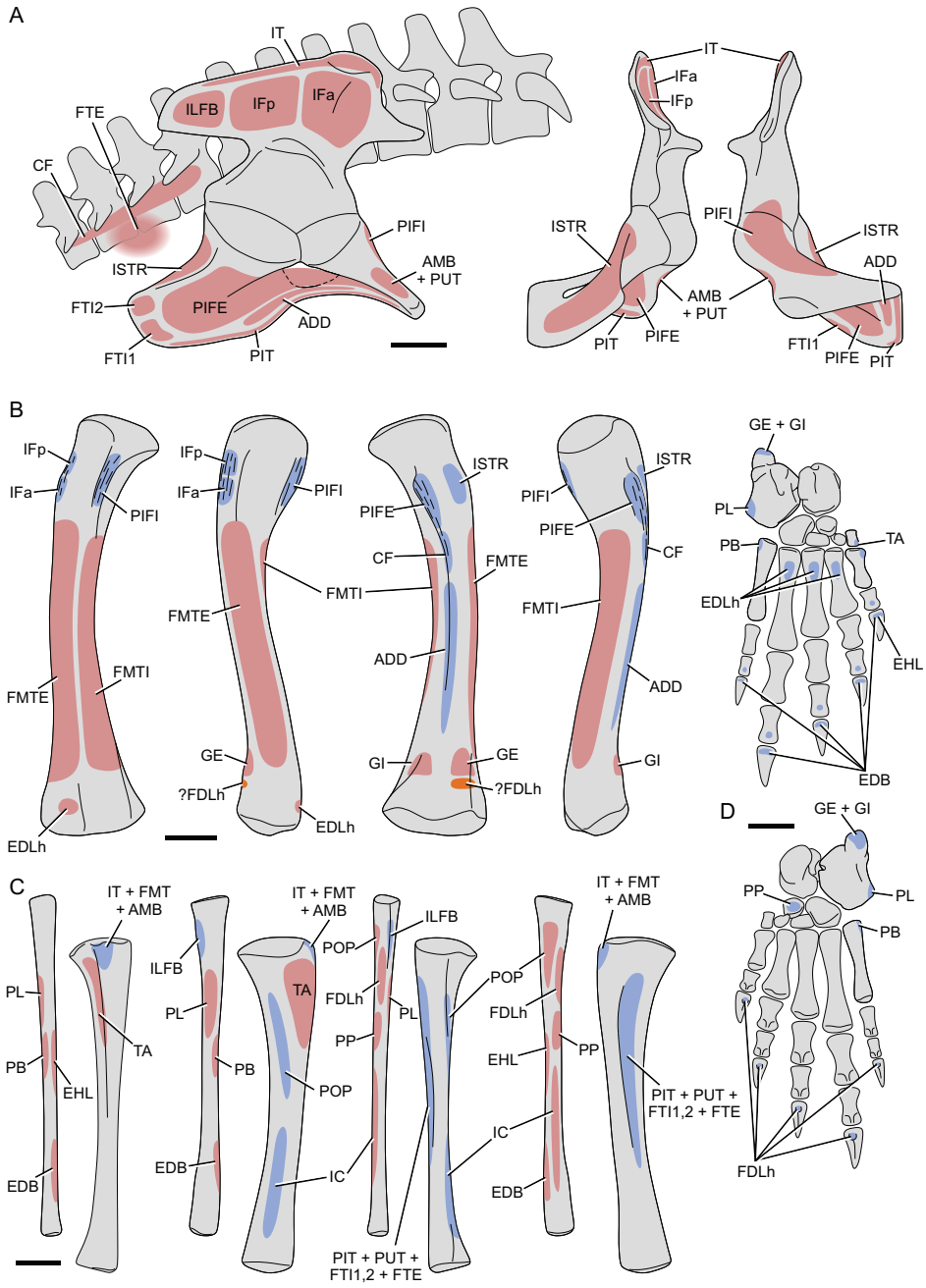

Figure 6. Reconstructed muscle attachments in *Regisaurus*. A, pelvis and axial skeleton, in lateral, posterior, and anterior views. B, femur in anterior, lateral, posterior, and medial views. C, tibia and fibula in anterior, lateral, posterior, and medial views. D, pes in dorsal (top) and ventral (bottom) views; phalangeal proportions based on SAM-PK-K10704 *Ictidosuchoides* cf. *longiceps*. Red denotes inferred origins, blue denotes inferred insertions, and orange denotes ambiguous attachments (see text). Scale = 10 mm. See Table 5 for muscle abbreviations.

TABLE 5. RECONSTRUCTED ORIGINS AND INSERTIONS IN *REGISAURUS JACOBI*. LOI, LEVEL OF INFERENCE IN THE SCHEME OF WITMER (1995).

		Origin		Insertion	
Muscle	Abbreviation	Attachment	LOI	Attachment	LOI
Iliotibialis	IT	Much of dorsal and anterior rim of iliac blade (thickened or rugose margin); via two heads	II	Tuberosity on anteroproximal end of cnemial crest of tibia, via common "triceps" tendon	I
Ambiens	AMB	Lateral aspect of pubis anteroventral to acetabulum, on or near pubic tubercle	II′	Tuberosity on anteroproximal end of cnemial crest of tibia, via common "triceps" tendon	I
Femorotibialis externus	FMTE	Lateral aspect of much of femoral shaft, distal to IF insertions	I′	Tuberosity on anteroproximal end of cnemial crest of tibia, via common "triceps" tendon	I
Femorotibialis internus	FMTI	Medial aspect of much of femoral shaft, distal and lateral to PIFI insertion	I′	Tuberosity on anteroproximal end of cnemial crest of tibia, via common "triceps" tendon	I
Iliofemoralis	IF	Much of lateral surface of preacetabular iliac blade, dorsal and anterior to acetabulum; via two heads	II′	Anterolateral aspect of greater trochanter on lateral proximal femur	II
Puboischiofemoralis internus	PIFI	Medial surface of the proximal pubis or ventral ilium; number of divisions uncertain	II′	Anteromedial aspect of proximal femur (longitudinal ridge with scarring)	II
Puboischiofemoralis externus	PIFE	Much of lateral surface of pubis and ischium surrounding obturator foramen; via two heads	II′	Posteromedial aspect of proximal femur, on internal trochanter (scarring)	II
Iliofibularis	ILFB	Lateral aspect of postacetabular iliac blade, posterior to IF origin and deep to IT origin	II	Anterolateral proximal fibula	II′
Flexor tibialis internus	FTI	Posterolateral ischium, with dorsal head (FTI2) originating on posterodorsal apex; via at least two heads	II′	Posteromedial tibia, in association with PIT and FTI insertions	II′
Flexor tibialis externus	FTE	Ilioischiadic ligament and fascia covering proximal tail	II′	Posteromedial tibia, in association with PIT and FTI insertions	II′
Puboischiotibialis	PIT	Ventral pubis and ischium along puboischiadic symphysis	II′	Longitudinal groove on medial tibia, in association with (and superficial to) FTI and FTE	II
Pubotibialis	PUT	Anterolateral pubis, on or near pubic tubercle; via singular head *OR* Anterolateral to anteroventral pubis near pubic tubercle; via two heads (pectineus [PECN] dorsally, adductor longus [ADDL] ventrally)	II′	Anteromedial to medial proximal tibia, in association with PIT and FTI (single head) *OR* Posteromedial aspect of much of femoral shaft (two heads)	II′

Table 5. Continued.

		Origin		Insertion	
Muscle	Abbreviation	Attachment	LOI	Attachment	LOI
Adductor femoris	ADD	Close to the puboischiadic suture on ventral pubis and ischium	II′	Posterior aspect of distal femoral shaft, along faint longitudinal ridge	II
Ischiotrochantericus	ISTR	Dorsolateral ischium (shallow, longitudinal depression facing dorsolaterally), plus medial surface of ischium	II	Posterior aspect of greater trochanter	II′
Caudofemoralis	CF	Transverse processes of posterior sacral vertebrae and proximalmost caudal vertebrae; via single head	II′	Posterior aspect of femoral shaft, distal to internal trochanter	II′
Gastrocnemius externus	GE	Posterolateral distal femur, proximal to lateral condyle	I′	Apex of calcaneal tuber	II
Gastrocnemius internus	GI	Posteromedial distal femur, proximal to medial condyle	II′	In common with GE	II
Flexor digitorum longus (hindlimb)	FDLh	Posteromedial aspect of head and proximal shaft of fibula	II′	Tendon that runs to insert on flexor tubercles of unguals	II
Flexor digitorum brevis	FDB	Dorsal (deep) surface of plantar fascia and adjacent tarsals and metatarsals	II′	Plantar aspect of proximal phalanges	II′
Extensor digitorum longus (hindlimb)	EDLh	Anterior aspect of distal femur proximal to lateral condyle	II′	Dorsal aspect of proximal metatarsals II–IV	II′
Extensor digitorum brevis (hindlimb)	EDBh	Anterior aspect of distal fibula	II′	Dorsal aspect of penultimate phalanges and extensor processes of unguals	I
Extensor hallucis longus	EHL	Anteromedial aspect of midshaft of fibula	II′	Extensor process on dorsal aspect of digit I ungual	II
Tibialis anterior	TA	Anterolateral aspect of proximal tibia, in lateral fossa of cnemial crest	II	Dorsomedial proximal aspect of entocuneiform or metatarsal I	II′
Peroneus longus	PL	Lateral proximal fibula, distal to ILFB insertion	II′	Distolateral shelf (“peroneal shelf”) of calcaneum	II
Peroneus brevis	PB	Anterolateral proximal fibula, anterior to PL origin	II′	Lateral aspect of base of metatarsal V	II′
Pronator profundus	PP	Posteromedial aspect of proximal fibular shaft, distal to FDLh origin	II′	Plantar aspect of navicular	II′
Popliteus	POP	Medial aspect of fibular head and proximal shaft	II	Posterolateral proximal tibia	II′
Interosseus cruris	IC	Medial aspect of distal fibular shaft	II′	Lateral aspect of distal tibial shaft	II′

or alternatively axial or costal musculature. The origin of the ITa is here reconstructed as on the anterodorsal iliac margin on the "main" part of the blade, but it is possible that it may have extended onto one of the anterior processes. In contrast, Kemp (1978) interpreted the origin in *Regisaurus* as near the anterior base of the ilium, rather like the mammalian RF, citing the presence of a shallow depression. However, such a structure may be a by-product of the strong development of the lower anterior iliac process in this taxon. Convincing osteological evidence for an RF-like origin in synapsids is not observed until advanced cynodonts (Bishop and Pierce, 2024b).

Character 12. As with *Oudenodon* and *Lycaenops*, the anteriorly expanded iliac surface area supports the reconstruction of two heads (state 1, level II′ inference).

Character 15. Without any positive evidence for a splitting of the muscle mass, the PIFI is conservatively reconstructed as singular here (state 0, level II′ inference).

Character 16. Eutherocephalians possess an anteroposteriorly abbreviated pubis, supporting the reconstruction of a restricted origin on the medial surface of the proximal pubis or ventral ilium (state 1, level II′ inference). Kemp (1978) reconstructed the origin on the ventral lateral aspect of the preacetabular iliac blade, in a comparable fashion to the iliac fossa of mammals; however, these structures are not phylogenetically continuous (i.e., nonhomologous), and such an inference is less well supported (state ~4, level III inference). As noted by Bishop and Pierce (2024b), the "fossa" recognized by Kemp may instead be a spandrel of the anterior iliac processes.

Character 18. Following the same line of reasoning as for *Oudenodon* and *Lycaenops*, the PIFE likely possessed some form of anteroposterior subdivision.

Character 27. Following the same line of reasoning as for *Oudenodon* and *Lycaenops*, an insertion on the tibia is reconstructed for *Regisaurus* (state 1, level II′ inference).

Character 28. The presence of the FTE is most parsimoniously inferred as a synapomorphy of Amniota (or a more inclusive clade), so only a single head is inferred for the FTE here (state 1, level II′ inference).

Character 29. The FTE was present in therocephalians (see previous character), but no osteological correlate of its origin is present (i.e., not states 0 or 3). The relatively "reptilian" arrangement of the pelvis (long postacetabular iliac blade, ischium well ventral to level of acetabulum) and lack of an ischiadic tuberosity imply a more "reptilian" (state 1 or 2) origin; in the absence of any scarring on the posterior ilium or ischium, the origin is reconstructed as from the ilioischiadic ligament and fascia covering the proximal tail (state 1, level II′ inference).

Character 31. Following the same line of reasoning as for *Oudenodon* and *Lycaenops*, a secondary attachment to the GL was absent in *Regisaurus* (state 2, level II′ inference).

Characters 34 and 35. Eutherocephalians are inferred to have exhibited a slight shift in PIFI origin (character 16, state 1). If Therocephalia is monophyletic, such a shift would probably have been convergent with that inferred in cynodonts, since scylacosaurids retained a well-developed (i.e., anteroposteriorly long) pubic plate (Boonstra, 1964), implying the retention of a plesiomorphic PUT. However, in a scenario of Therocephalian paraphyly, where eutherocephalians are more closely related to cynodonts (see Bishop and Pierce, 2024b), a PIFI origin shift is phylogenetically congruent with the inferred shift on the stem lineage, wherein PUT reorganization in eutherocephalians becomes more likely. In the absence of other osteological evidence, it is currently not possible to discriminate between the plesiomorphic (state 0) and derived (state 2) conditions.

Character 37. As the ADD is unambiguously reconstructed as possessing a single head (character 36), this obviates the possibility of a

crocodylian-like origin. However, it is not possible to discern between the remaining potential states in the absence of osteological evidence. As the puboischiadic plate is markedly transformed in eutherocephalians (paralleling the same transformation in cynodonts), the more mammalian condition is tentatively inferred in *Regisaurus* (state 3, level II′ inference), reconstructing the origin at the ventral junction of the pubis and ischium.

Character 43. The greatly reduced tail of eutherocephalians (Kemp, 1986; Fourie and Rubidge, 2007) suggests a more mammalian type of origin for the CF. The condition observed in monotremes is reconstructed here for *Regisaurus*, whereby an osseous contact is still retained (state 2, level II′ inference).

Character 46. The gastrocnemii are ubiquitous among amniotes, and so the GE can be confidently inferred as present in eutherocephalians. The development of a distinct calcaneal tuber in many baurioid eutherocephalians (including *Regisaurus*) may be argued to signal increasing differentiation into multiple heads, but extant crocodylians also possess a calcaneal tuber and an undivided GE. Even in well-preserved, articulated skeletons (e.g., BP/1/3973 *Olivierosuchus parringtoni*, SAM-PK-K10704 *Ictidosuchoides* cf. *longiceps*), there is no evidence for ossified fabellae, or a parafibula, which might signal subdivisions. Without any positive evidence for a splitting of the muscle mass, the GE is conservatively reconstructed as singular here (state 1, level II′ inference).

Character 48. As per character 46, a distinct PLA was not present in *Regisaurus* (state 0, level II′ inference).

Character 52. As per character 46, a distinct PLA was not present in *Regisaurus* (state 0, level II′ inference).

Character 55. The locus of the FDLh origin in amniotes is generally centered around the posterior proximal fibula; this area is conservatively reconstructed as the primary attachment for the FDLh in *Regisaurus* (state ~3, level II′ inference; parafibula is unknown in non-cynodont therapsids).

Character 56. Baurioids including *Regisaurus* can be explicitly coded for state 1 here as they possess a distinct calcaneal tuber (state 1, level II inference).

Character 61. Following the same logic as outlined above for *Oudenodon* and *Lycaenops*, the attachment in *Regisaurus* is assumed to be centered on the femur (approximating state 1, level II′ inference).

Character 62. In the absence of any positive osteological evidence, the plesiomorphic state is reconstructed here for *Regisaurus* (state 0, level II′ inference).

Character 64. Following the same logic as outlined above for *Oudenodon* and *Lycaenops*, the EDBh in *Regisaurus* is reconstructed as originating from the anterior aspect of the distal fibula (state 2, level II′ inference).

Character 66. Following the same logic as outlined above for *Oudenodon* and *Lycaenops*, the origin of the EHL in *Regisaurus* is reconstructed at the fibular midshaft (state 2, level II′ inference).

Character 69. An insertion of the TA distal to the ankle is ubiquitous among amniotes, with the general locus of attachment located at metatarsal I. Therocephalians already had achieved the tarsal arrangement observed in extant mammals (Schaeffer, 1941; Boonstra, 1964; Kemp, 1986; personal obsservation of BP and SAM specimens), suggesting that *Regisaurus* likely possessed a more mammal-like attachment of the TA, on the entocuneiform in addition to metatarsal I (state 3, level II′ inference).

Character 71. Following the same logic as outlined above for *Oudenodon* and *Lycaenops*, the PL in *Regisaurus* is inferred to have originated from around the proximal fibula (state 3, level II′ inference).

Character 72. Following the same logic as outlined above for *Oudenodon* and *Lycaenops*, the PB likely originated from the anterolateral proximal fibula in *Regisaurus* (state 3, level II′ inference).

Character 74. Following the same logic as outlined above for *Oudenodon* and *Lycaenops*, the PB of *Regisaurus* likely inserted on metatarsal V (state 4, level II′ inference).

Character 76. Therocephalians already had achieved the tarsal arrangement observed in extant mammals, suggesting that *Regisaurus* may have possessed a more mammal-like attachment of the PP on the plantar aspect of the proximal tarsals (state 3, level II′ inference).

Massetognathus pascuali

The reconstruction presented in Figure 7 is based principally on MCZ VPRA-3691, which comprised the disarticulated skeletons of several individuals and one additional individual that remains nearly fully articulated (Jenkins, 1970). Additional material of *Massetognathus* in the MCZ and PVL collections helped refine observations and inferences. Phalangeal morphology is principally based on *Thrinaxodon liorhinus* (Fernandez et al., 2013). Inferred origins and insertions are described in Table 6. *Massetognathus* was codified as part of Cynognathia, and reconstructed states at the node Eucynodontia (Table S6) were used to clarify remaining uncertainties. Some character states remained ambiguous for this node, and these were resolved for *Massetognathus* as follows.

Character 2. Although the state is unambiguous for *Massetognathus*, the exact location on the ilium is ambiguous, given the uncertainty in precisely when the migration of the ITa to RF took place. The origin is tentatively reconstructed on the anterior margin of the ilium, but it is possible that it may have already become more ventrally situated by the appearance of Eucynodontia.

Character 12. The apomorphic anterior expansion of the cynodont iliac blade suggests enlargement and probable differentiation of the primitive iliofemoralis mass, and so two heads are conservatively reconstructed here (state 1, level II′ inference).

Character 15. Without any positive evidence for a splitting of the muscle mass, the PIFI is conservatively reconstructed as singular here (state 0, level II′ inference).

Character 18. There is no positive evidence for a splitting of the PIFE muscle mass in cynodonts, and conservatively a single head would be reconstructed. However, as explained for the non-cynodont therapsids, the relatively broad area of the inferred origin (character 19) suggests that the PIFE likely possessed some form of anteroposterior subdivision, correlating with the mammalian OBEX (anterior) and QF (posterior).

Character 27. Following the same line of reasoning as for the therapsids, an insertion on the tibia is reconstructed for *Massetognathus* (state 1, level II′ inference).

Character 28. The presence of the FTE is most parsimoniously inferred as a synapomorphy of Amniota (or a more inclusive clade), so only a single head is inferred for the FTE here (state 1, level II′ inference).

Character 29. As per the previous character, the FTE is inferred as present. The appearance of the ischiadic tuberosity in eucynodonts potentially signaled a topographic shift/reorganization of the crural flexor musculature (Bishop and Pierce, 2024b), whereby the FTE shifted from dorsal to the ischium to becoming more strongly associated with the ischium. To this end, an origin from near the ischiadic tuberosity is inferred here for *Massetognathus* (state 3, level II′ inference), occupying a position corresponding more closely to the posterior (ventral) division of crown mammals.

Character 31. Following the same line of reasoning as for the therapsids, a secondary attachment to the GL was absent in *Massetognathus* (state 2, level II′ inference).

Character 34. Cynodonts are inferred to have already exhibited a shift in PIFI origin (character 16, state 2), which in turn suggests a change in PUT topology from the plesiomorphic, single-headed condition (see Bishop and Pierce, 2024b). Two heads and two origins are reconstructed in

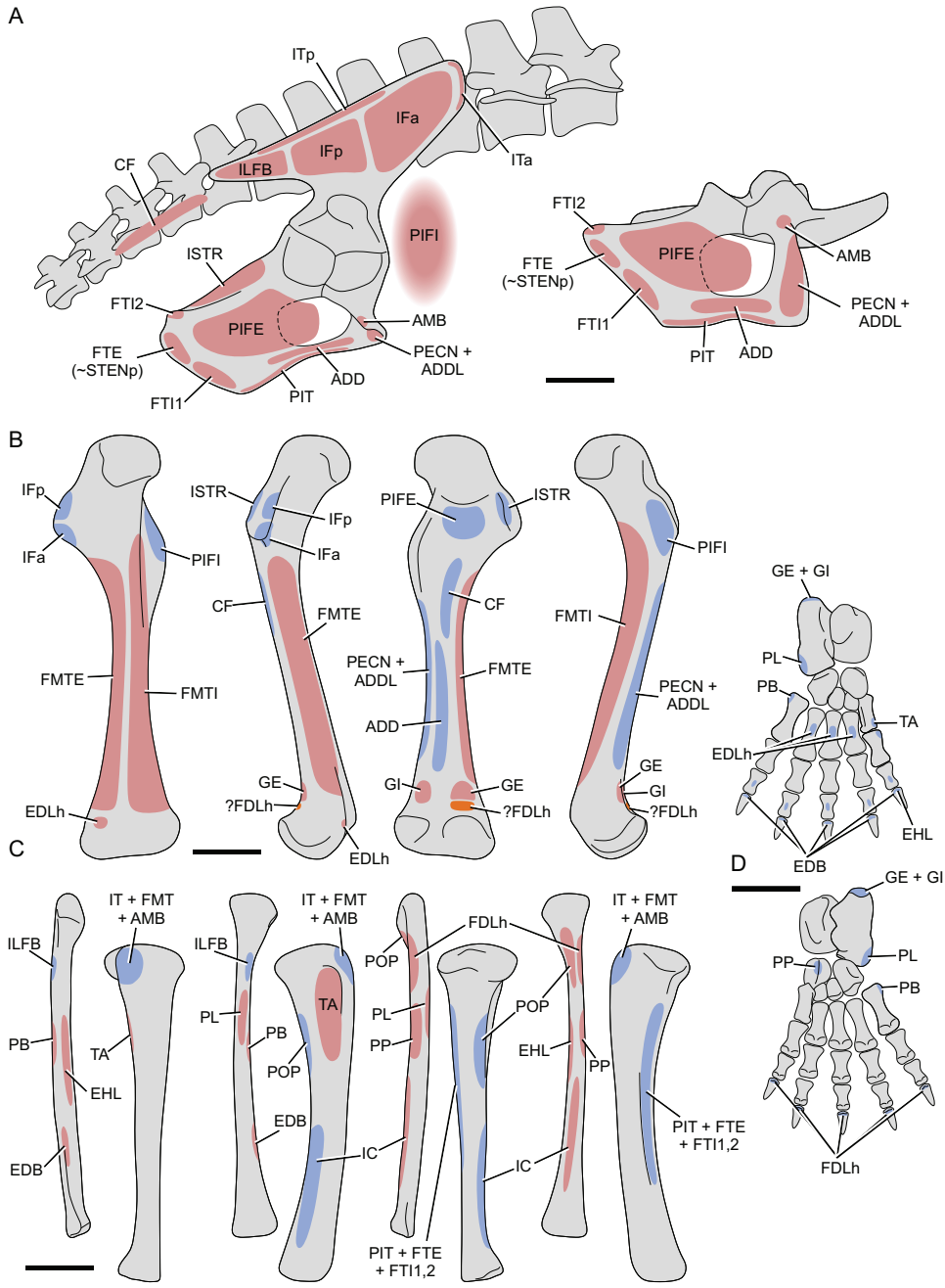

Figure 7. Reconstructed muscle attachments in *Massetognathus*. A, pelvis and axial skeleton, in lateral and ventral views. B, femur in anterior, lateral, posterior, and medial views. C, tibia and fibula in anterior, lateral, posterior, and medial views. D, pes in dorsal (top) and ventral (bottom) views; phalanges based in *Thrinaxodon*. Red denotes inferred origins, blue denotes inferred insertions, and orange denotes ambiguous attachments (see text). Scale = 10 mm. See Table 6 for muscle abbreviations.

TABLE 6. RECONSTRUCTED ORIGINS AND INSERTIONS IN *MASSETOGNATHUS PASCUALI*. LOI, LEVEL OF INFERENCE IN THE SCHEME OF WITMER (1995).

		Origin		Insertion	
Muscle	Abbreviation	Attachment	LOI	Attachment	LOI
Iliotibialis	IT	Much of dorsal and anterior rim of iliac blade (thickened or rugose margin); via two heads	II	Tuberosity on anteroproximal end of cnemial crest of tibia, via common "triceps" tendon	I
Ambiens	AMB	Lateral aspect of pubis anteroventral to acetabulum, on or near pubic tubercle	II′	Tuberosity on anteroproximal end of cnemial crest of tibia, via common "triceps" tendon	I
Femorotibialis externus	FMTE	Lateral aspect of much of femoral shaft, distal to IF insertions	I′	Tuberosity on anteroproximal end of cnemial crest of tibia, via common "triceps" tendon	I
Femorotibialis internus	FMTI	Medial aspect of much of femoral shaft, distal and lateral to PIFI insertion	I′	Tuberosity on anteroproximal end of cnemial crest of tibia, via common "triceps" tendon	I
Iliofemoralis	IF	Much of lateral surface of preacetabular iliac blade, dorsal and anterior to acetabulum; via two heads	II′	Anterolateral aspect of greater trochanter on lateral proximal femur	II
Puboischiofemoralis internus	PIFI	Dorsal surface of anteromedial pubis and/or ventromedial surface of preacetabular iliac blade; number of divisions uncertain	II′	Anteromedial aspect of lesser trochanter on medial proximal femur	II
Puboischiofemoralis externus	PIFE	Much of lateral surface of pubis and ischium surrounding obturator foramen; via two heads	II′	Posterior proximal femur in gentle depression between greater and lesser trochanters	II′
Iliofibularis	ILFB	Lateral aspect of postacetabular iliac blade, posterior to IF origin and deep to IT origin	II	Tubercle on anterolateral proximal fibula	II
Flexor tibialis internus	FTI	Posterolateral ischium, with dorsal head originating on ischiadic tuberosity on posterodorsal apex (FTI2 = BICF); via at least two heads	II	Posteromedial tibia, in association with PIT and FTE insertions	II′
Flexor tibialis externus	FTE	Posterolateral ischium in neighborhood of ischiadic tuberosity	II′	Posteromedial tibia, in association with PIT and FTI insertions	II′
Puboischiotibialis	PIT	Ventral pubis and ischium along puboischiadic symphysis	II′	Longitudinal groove on medial tibia, in association with (and superficial to) FTI and FTE	II
Pubotibialis	PUT	Anterolateral to anteroventral pubis near pubic tubercle; via two heads (pectineus [PECN] dorsally, adductor longus [ADDL] ventrally)	II′	Posteromedial aspect of much of femoral shaft	II′
Adductor femoris	ADD	Close to the puboischiadic suture on ventral pubis and ischium	II′	Posterior aspect of distal femoral shaft	II′

Table 6. Continued.

Muscle	Abbreviation	Origin		Insertion	
		Attachment	LOI	Attachment	LOI
Ischiotrochantericus	ISTR	Dorsolateral ischium (shallow, longitudinal depression facing dorsolaterally), plus medial surface of ischium	II	Posteriorly expanded apex of greater trochanter	II′
Caudofemoralis	CF	Transverse processes of posterior sacral vertebrae and proximalmost caudal vertebrae; via single head	II′	Posterior aspect of femoral shaft, distal to PIFE insertion	II′
Gastrocnemius externus	GE	Posterolateral distal femur, proximal to lateral condyle	I′	Apex of calcaneal tuber	II
Gastrocnemius internus	GI	Posteromedial distal femur, proximal to medial condyle	II′	In common with GE	II
Flexor digitorum longus (hindlimb)	FDLh	Posteromedial aspect of head and proximal shaft of fibula	II′	Tendon that runs to insert on flexor tubercles of unguals	II
Flexor digitorum brevis	FDB	Dorsal (deep) surface of plantar fascia and adjacent tarsals and metatarsals	II′	Plantar aspect of proximal phalanges	II′
Extensor digitorum longus (hindlimb)	EDLh	Anterior aspect of distal femur proximal to lateral condyle	II′	Dorsal aspect of proximal metatarsals II–IV	II′
Extensor digitorum brevis (hindlimb)	EDBh	Anterior aspect of distal fibula	II′	Dorsal aspect of penultimate phalanges and extensor processes of unguals	I
Extensor hallucis longus	EHL	Anteromedial aspect of midshaft of fibula	II′	Extensor process on dorsal aspect of digit I ungual	II
Tibialis anterior	TA	Anterolateral aspect of proximal tibia, in lateral fossa of cnemial crest	II	Dorsomedial proximal aspect of entocuneiform or metatarsal I	II′
Peroneus longus	PL	Lateral proximal fibula, distal to ILFB insertion	II′	Distolateral shelf ("peroneal shelf") of calcaneum	II
Peroneus brevis	PB	Anterolateral proximal fibula, anterior to PL origin	II′	Lateral aspect of base of metatarsal V	II′
Pronator profundus	PP	Posteromedial aspect of proximal fibular shaft, distal to FDLh origin	II′	Plantar aspect of navicular	II′
Popliteus	POP	Medial aspect of fibular head and proximal shaft	II	Posterolateral proximal tibia	II′
Interosseus cruris	IC	Medial aspect of distal fibular shaft	II′	Lateral aspect of distal tibial shaft	II′

here in *Massetognathus* (state 2, level II′ inference).

Character 35. Following the same logic as for the preceding character, two femoral insertions are reconstructed in *Massetognathus* (state 2, level II′ inference), corresponding to the PECN and ADDL.

Character 37. As the ADD is unambiguously reconstructed as possessing a single head (character 36), this obviates the possibility of a crocodylian-like origin. However, it is not possible to discern between the remaining potential states in the absence of osteological evidence. As the puboischiadic plate is already markedly transformed in eucynodonts, the more mammalian condition is tentatively inferred in *Massetognathus* (state 3, level II′ inference), reconstructing

the origin at the ventral junction of the pubis and ischium.

Character 43. The greatly reduced tail of cynodonts, including *Massetognathus* (Jenkins, 1970), suggests a more mammalian type of origin for the CF. The monotremes' condition is reconstructed here for *Massetognathus*, whereby an osseous contact is still retained (state 2, level II′ inference).

Character 46. The gastrocnemii are ubiquitous among amniotes, and so the GE can be confidently inferred as present in cynodonts. The development of a distinct calcaneal tuber in cynodonts (including *Massetognathus*) may signal increasing differentiation into multiple heads, but crocodylians also possess a calcaneal tuber and an undivided GE. Even in well-preserved, articulated skeletons of cynodonts (including those of *Massetognathus*), there is no evidence for ossified fabellae, or a parafibula, which might signal subdivisions. Without any positive evidence for a splitting of the muscle mass, the GE is conservatively reconstructed as singular here (state 1, level II′ inference).

Character 48. As per character 46, a distinct PLA was not present in *Massetognathus* (state 0, level II′ inference).

Character 52. As per character 46, a distinct PLA was not present in *Massetognathus* (state 0, level II′ inference).

Character 55. The locus of the FDLh origin in amniotes is generally centered around the posterior proximal fibula; this area is conservatively reconstructed as the primary attachment for the FDLh in *Massetognathus* (state ~3, level II′ inference; parafibula is unknown in basal cynodonts).

Character 61. Following the same logic as outlined above for the therapsids, the attachment in *Massetognathus* is assumed to be centered on the femur (approximating state 1, level II′ inference).

Character 62. In the absence of any positive osteological evidence, the plesiomorphic state is conservatively reconstructed here for *Massetognathus* (state 0, level II′ inference).

Character 64. Following the same logic as outlined above for the therapsids, the EDBh in *Massetognathus* is reconstructed as originating from the anterior aspect of the distal fibula (state 2, level II′ inference).

Character 66. Following the same logic as outlined above for the therapsids, the origin of the EHL in *Massetognathus* is reconstructed at the fibular midshaft (state 2, level II′ inference). Jenkins (1971, fig. 58) described a ridge on the anterior fibula of *Cynognathus* (or *Diademodon*), which may signify the attachment of this muscle in that taxon.

Character 69. An insertion of the TA distal to the ankle is ubiquitous among amniotes, with the general locus of attachment located at metatarsal I. Cynodonts already had achieved the tarsal arrangement observed in extant mammals (Bonaparte, 1963; Jenkins, 1971; De Oliveira et al., 2010; Fernandez et al., 2013; Liu et al., 2017), suggesting that *Massetognathus* may have possessed a more mammal-like attachment of the TA, on the entocuneiform in addition to metatarsal I (state 3, level II′ inference).

Character 71. Following the same logic as outlined above for the therapsids, the PL in *Massetognathus* is inferred to have originated from around the proximal fibula (state 3, level II′ inference).

Character 72. Following the same logic as outlined above for the therapsids, the PB likely originated from the anterolateral proximal fibula in *Massetognathus* (state 3, level II′ inference).

Character 74. Following the same logic as outlined above for the therapsids, the PB of *Massetognathus* likely inserted on metatarsal V (state 4, level II′ inference).

Character 76. Cynodonts already had achieved the tarsal arrangement observed in extant mammals, suggesting that *Massetognathus* may have possessed a more mammal-like attachment of the PP on the plantar aspect of the proximal tarsals (state 3, level II′ inference).

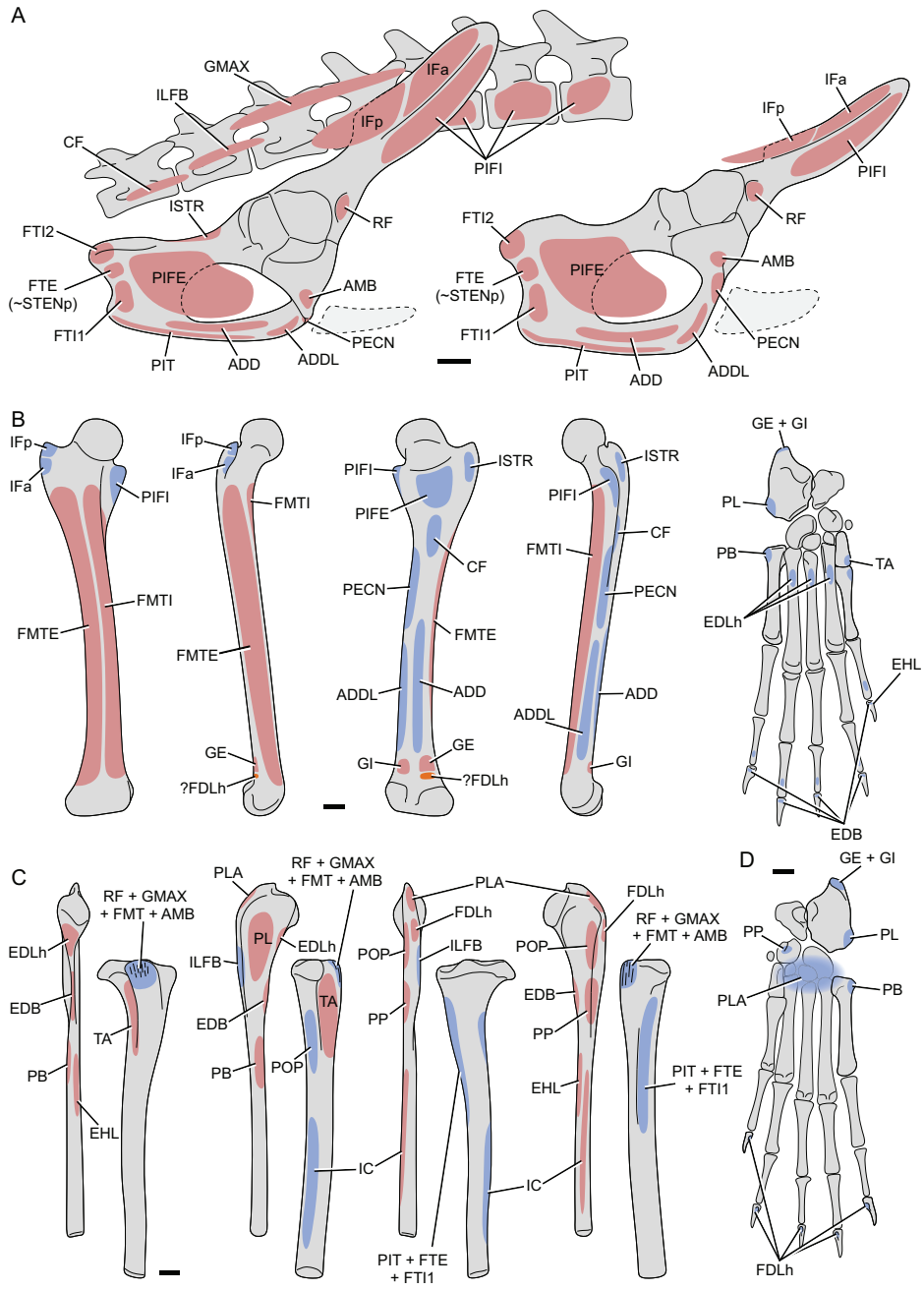

Figure 8. Reconstructed muscle attachments in *Megazostrodon.* A, pelvis and axial skeleton, in lateral and ventrolateral views; although unknown from fossils, an epipubis (dashed outline) was possibly present in *Megazostrodon.* B, femur in anterior, lateral, posterior, and medial views. C, tibia and fibula in anterior, lateral, posterior, and medial views. D, pes in dorsal (top) and ventral (bottom) views. Red denotes inferred origins, blue denotes inferred insertions, and orange denotes ambiguous attachments (see text). Scale = 1 mm. See Table 7 for muscle abbreviations.

Megazostrodon rudnerae

The reconstruction presented in Figure 8 is based principally on the holotype, NHMUK PV M.26407, a partially articulated individual for which the postcranial elements were originally described by Jenkins and Parrington (1976). The pubis, proximal tibia, distal tibia and fibula, and a few pedal elements are missing, so those parts of the anatomy were based on the closely related morganucodontids *Erythrotherium parringtoni* and *Eozostrodon parvus*. In addition to the descriptions provided by Jenkins and Parrington (1976), information on both taxa was also sought from firsthand observation of material (SAM-PK-K359 for *Erythrotherium*, and various specimens in the MCZ collections for *Eozostrodon*). Inferred origins and insertions are described in Table 7. *Megazostrodon* was codified as part of Morganucodontidae, and reconstructed states at the node Mammaliaformes (Table S7) were used to clarify remaining uncertainties. Some character states remained ambiguous for this node, and these were resolved for *Megazostrodon* as follows.

Character 12. Following the same logic as for *Massetognathus*, two heads are conservatively reconstructed here for *Megazostrodon* (state 1, level II′ inference). The development of a longitudinal ridge and gluteal fossa on the ilium of derived probainognathian cynodonts also suggests that this part of the hindlimb had closely approached the mammalian condition, further supporting the inference of multiple heads here.

Character 15. Without any positive evidence for a splitting of the muscle mass, the PIFI is conservatively reconstructed as singular here (state 0, level II′ inference; an "iliopsoas").

Character 18. There is no positive evidence for a splitting of the muscle mass in probainognathians, and conservatively a single head would be reconstructed. However, the inferred origin (character 19) nonetheless covers a broad area, and so in a similar fashion to *Massetognathus*, an anteroposterior subdivision is considered plausible (state 1, level II′ inference).

Character 27. The FTI2 is synapomorphic for Amniota (character 23), and so it can be inferred to have existed in *Megazostrodon*. As hypothesized by Bishop and Pierce (2024b), the persistence of a fibular ridge suggests that the switch from ILFB-dominated (TEN-dominated) to FTI2-dominated (BICF-dominated) attachment on the fibula probably occurred crownward of Mammaliaformes. Nevertheless, not that further up the stem lineage at crown Mammalia, the BICF dominates the lateral attachment. It is therefore probable that an intermediary or transitional attachment on the posterior fascia of the crus existed in *Megazostrodon* (state 1/2, level II′ inference; cf. Romer, 1922, plate 39).

Character 28. The presence of the FTE is most parsimoniously inferred as a synapomorphy of Amniota (or a more inclusive clade), so only a single head is inferred for the FTE here (state 1, level II′ inference).

Character 29. Following the line of reasoning outlined for *Massetognathus*, an origin from near the ischiadic tuberosity is inferred here for *Megazostrodon* (state 3, level II′ inference). The tuberosity is well developed in morganucodontids, including *Megazostrodon*.

Character 31. Following the same line of reasoning as for *Massetognathus*, a secondary attachment to the GL was absent in *Megazostrodon* (state 2, level II′ inference).

Character 34. Following the same logic as for *Massetognathus*, a shift in PIFI origin and PUT recombination are inferred to have taken place prior to Mammaliaformes. The presence of the typical "trihedral" iliac structure in morganucodontids (first appearing around *Prozostrodon*) supports the inference of a typically mammalian configuration, and two heads and two origins are therefore reconstructed in *Megazostrodon* (state 2, level II′ inference; PECN and ADDL).

TABLE 7. RECONSTRUCTED ORIGINS AND INSERTIONS IN *MEGAZOSTRODON RUDNERAE*. LOI, LEVEL OF INFERENCE IN THE SCHEME OF WITMER (1995).

		Origin		Insertion	
Muscle	Abbreviation	Attachment	LOI	Attachment	LOI
Iliotibialis	IT	Base of ilium, immediately anterior to acetabulum (rectus femoris [RF], pit); and sacral and proximalmost caudal vertebrae (gluteus maximus [GMAX])	II	Tuberosity on anteroproximal end of cnemial crest of tibia, via common "triceps" tendon	I
Ambiens	AMB	Lateral aspect of pubis anteroventral to acetabulum, on or near pubic tubercle	II′	Tuberosity on anteroproximal end of cnemial crest of tibia, via common "triceps" tendon	I
Femorotibialis externus	FMTE	Lateral aspect of much of femoral shaft, distal to IF insertions	I′	Tuberosity on anteroproximal end of cnemial crest of tibia, via common "triceps" tendon	I
Femorotibialis internus	FMTI	Medial aspect of much of femoral shaft, distal and lateral to PIFI insertion	I′	Tuberosity on anteroproximal end of cnemial crest of tibia, via common "triceps" tendon	I
Iliofemoralis	IF	Shallow gluteal fossa occupying dorsal half of iliac blade (possibly extending posteriorly over last sacral or first caudal vertebra); via two heads	II	Anterolateral aspect of greater trochanter on lateral proximal femur	II
Puboischiofemoralis internus	PIFI	Shallow iliac fossa occupying ventral half of iliac blade, extending onto sacral or posteriormost lumbar vertebrae; number of divisions uncertain	II	Anteromedial aspect of lesser trochanter on medial proximal femur	II
Puboischiofemoralis externus	PIFE	Much of lateral surface of pubis and ischium surrounding obturator foramen; via two heads, one anterior (obturator externus [OBEX]) and one posterior (quadratus femoris [QF])	II′	Posterior proximal femur in depression between greater and lesser trochanters	II′
Iliofibularis	ILFB	Transverse processes of anterior caudal vertebrae, deep to posterior IT origin (no postacetabular ilium)	II	Ridge on posterolateral proximal fibula	II
Flexor tibialis internus	FTI	Posterolateral ischium, with dorsal head originating on ischiadic tuberosity on posterodorsal apex (FTI2 = BICF); via at least two heads	II	Posteromedial tibia, in association with PIT and FTE insertions (FTI1) and fascia of posterior crus (FTI2)	II′

TABLE 7. CONTINUED.

		Origin		Insertion	
Muscle	Abbreviation	Attachment	LOI	Attachment	LOI
Flexor tibialis externus	FTE	Posterolateral ischium in neighborhood of ischiadic tuberosity	II′	Posteromedial tibia, in association with PIT and FTI insertions	II′
Puboischiotibialis	PIT	Ventral pubis and ischium along puboischiadic symphysis	II′	Longitudinal groove on medial tibia, in association with (and superficial to) FTI and FTE	II
Pubotibialis	PUT	Anterolateral to anteroventral pubis near pubic tubercle; via two heads (pectineus [PECN] dorsally, adductor longus [ADDL] ventrally)	II′	Posteromedial aspect of much of femoral shaft	II′
Adductor femoris	ADD	Close to the puboischiadic suture on ventral pubis and ischium	II′	Posterior aspect of distal femoral shaft	II′
Ischiotrochantericus	ISTR	Dorsal ischium (distinct squared-off surface facing dorsally), plus medial surface of ischium	II	Posterior aspect of greater trochanter	II′
Caudofemoralis	CF	Transverse processes of proximal caudal vertebrae; via single head	II′	Posterior aspect of femoral shaft, distal to PIFE insertion	II′
Gastrocnemius externus	GE	Posterolateral distal femur, proximal to lateral condyle	I′	Apex of calcaneal tuber	II
Gastrocnemius internus	GI	Posteromedial distal femur, proximal to medial condyle	II′	In common with GE	II
Plantaris	PLA	Posterior aspect of parafibular process on proximal fibula	II	Plantar fascia on ventral aspect of pes, possibly continuing on to tarsals or metatarsals	II′
Flexor digitorum longus (hindlimb)	FDLh	Parafibular process on proximal fibula	II′	Tendon that runs to insert on flexor tubercles of unguals	II
Flexor digitorum brevis	FDB	Dorsal (deep) surface of plantar fascia and adjacent tarsals and metatarsals	II′	Plantar aspect of proximal phalanges	II′
Extensor digitorum longus (hindlimb)	EDLh	Anterior aspect of proximal fibula	II′	Dorsal aspect of proximal metatarsals II–IV	II′
Extensor digitorum brevis (hindlimb)	EDBh	Anterior aspect of proximal fibula, distal to EDLh origin	II′	Dorsal aspect of penultimate phalanges and extensor processes of unguals	I
Extensor hallucis longus	EHL	Anteromedial aspect of midshaft of fibula	II′	Extensor process on dorsal aspect of digit I ungual	II
Tibialis anterior	TA	Anterolateral aspect of proximal tibia, in lateral fossa of cnemial crest	II	Dorsomedial proximal aspect of entocuneiform or metatarsal I	II′
Peroneus longus	PL	Lateral proximal fibula, in large fossa	II′	Distolateral shelf ("peroneal shelf") of calcaneum	II
Peroneus brevis	PB		II′		II′

Table 7. Continued.

Muscle	Abbreviation	Origin		Insertion	
		Attachment	LOI	Attachment	LOI
		Anterolateral proximal fibula, anterior to PL origin		Lateral aspect of base of metatarsal V	
Pronator profundus	PP	Posteromedial aspect of proximal fibular shaft, distal to expanded head	II′	Plantar aspect of navicular	II′
Popliteus	POP	Posteromedial aspect of fibular head, proximal to PP origin	II	Posterolateral proximal tibia	II′
Interosseus cruris	IC	Medial aspect of distal fibular shaft	II′	Lateral aspect of distal tibial shaft	II′

Character 35. Following the same logic as for the preceding character, two femoral insertions are reconstructed in *Megazostrodon* (state 2, level II′ inference), corresponding to the PECN and ADDL.

Character 37. As the ADD is unambiguously reconstructed as possessing a single head (character 36), this obviates the possibility of a crocodylian-like origin. However, it is not possible to discern between the remaining potential states in the absence of osteological evidence. As the puboischiadic plate of morganucodontids is essentially mammalian in gross structure (posteriorly swept pubis, large obturator fenestra, narrow puboischiadic rami), the mammalian condition is tentatively inferred in *Megazostrodon* (state 3, level II′ inference), with the origin reconstructed at the ventral junction of the pubis and ischium.

Character 43. NHMUK PV M.26407 preserves at least five well-developed caudal vertebrae in articulation with the sacrum, and Jenkins and Parrington (1976) interpreted the tail of *Eozostrodon* to comprise at least 12 vertebrae. The tail of morganucodontids was therefore of moderate length, albeit apparently thin in relation to the rest of the animal. The monotremes' condition is reconstructed here for *Megazostrodon*, whereby an osseous contact is still retained (state 2, level II′ inference).

Character 46. The gastrocnemii are ubiquitous among amniotes, and so the GE can be confidently inferred as present in morganucodontids. The development of an incipient parafibula is taken to indicate the differentiation of the PLA (character 48), but it is assumed here that the SOL is an apomorphy of Theria (or a more inclusive clade, e.g., Theriiformes), thus leading to state 2 being reconstructed here (level II′ inference).

Character 52. As per character 48, the PLA is inferred as present in *Megazostrodon*, although the exact manner of the insertion of this muscle, distal to the plantar fascia, is not certain (states 1/2, level II′ inference).

Character 55. The locus of the FDLh origin in amniotes is generally centered around the posterior proximal fibula; this area is conservatively reconstructed as the primary attachment for the FDLh in *Megazostrodon*. The presence of an incipient parafibula suggests that a more monotreme-like condition existed here (state ~2, level II′ inference).

Character 61. The locus of the EDLh origin in amniotes is generally centered around the anterior knee region, with mammals typically involving more of the fibula or tibia than the femur. Given the modifications to the fibula prior to Mammaliaformes (i.e., spatulate shape, incipient parafibula),

this suggests significant reorganization of the associated soft tissues as well; consequently, the origin is reconstructed as from the anterior aspect of the fibular head (state ~2, level II′ inference), distal to the knee.

Character 62. In the absence of any positive osteological evidence, the plesiomorphic state is reconstructed here for *Megazostrodon* (state 0, level II′ inference), although its close phylogenetic proximity to mammals may argue for state 1 being more likely instead.

Character 64. Plesiomorphically, the general locus of the origin for the EDBh is the ankle joint, but extant mammals exhibit an origin near the proximal fibula. The close phylogenetic proximity to mammals and the presence of an incipient parafibula in morganucodontids suggest that the mammalian configuration is the most likely configuration (state 3, level II′ inference). The muscle's proximal path is therefore reconstructed as along the anterior face of the fibula, rather than between fibula and tibia, to reflect the muscle approaching a more "mammalian" position; however, since a lateral malleolus is unknown in morganucodontids, the path probably was not yet on the extreme lateral aspect of the fibula.

Character 66. Following the same logic as outlined above for *Massetognathus*, the origin of the EHL in *Megazostrodon* is reconstructed at the fibular midshaft (state 2, level II′ inference). Extension of the origin onto the parafibula or medial tibia is apomorphic for one genus of monotreme or another (Gambaryan et al., 2002), and so it is not phylogenetically informative.

Character 69. An insertion of the TA distal to the ankle is ubiquitous among amniotes, with the general locus of attachment located at metatarsal I. *Megazostrodon* possessed the same tarsal arrangement observed in extant mammals, suggesting that it possessed a more mammal-like attachment of the TA, on the entocuneiform in addition to metatarsal I (state 3, level II′ inference).

Character 71. The PL can unambiguously be inferred to have originated from around the lateral knee region, but specifically where cannot be discerned. The more mammalian construction of the bones (especially fibula) around the knee joint in *Megazostrodon* supports a more mammalian manifestation of muscle attachment being present. To that end, an origin from the lateral proximal fibula is reconstructed here (state 3, level II′ inference), where a large fossa provides ample area for attachment.

Character 72. Following the same logic as outlined above for *Massetognathus*, the PB likely originated from the anterolateral proximal fibula in *Megazostrodon* (state 3, level II′ inference).

Character 74. Following the same logic as outlined above for *Massetognathus*, the PB of *Megazostrodon* likely inserted on metatarsal V (state 4, level II′ inference).

Character 76. Cynodonts already had achieved the tarsal arrangement observed in extant mammals, suggesting that *Megazostrodon* possessed a more mammal-like attachment of the PP on the plantar aspect of the proximal tarsals (state 3, level II′ inference).

Vincelestes neuquenianus

The reconstruction presented in Figure 9 is based on material belonging to several similarly sized individuals in the MACN collections, found together as multiple associated and disarticulated skeletons (Rougier, 1993). These specimens collectively comprise all pelvic and hindlimb elements except the distal tarsals, metatarsals, and phalanges, which are poorly represented in the available material. Anatomy of the distal pes was thus based on the more completely known pedes of *Jeholodens jenkinsi* (Ji et al., 1999), *Zhangheotherium quinquecuspidens* (Luo and Ji, 2005), *Akidolestes cifellii* (Chen and Luo, 2013), and *Henkelotherium guimarotae* (Krebs, 1991; Jäger et al., 2019). Inferred origins and insertions are described in Table

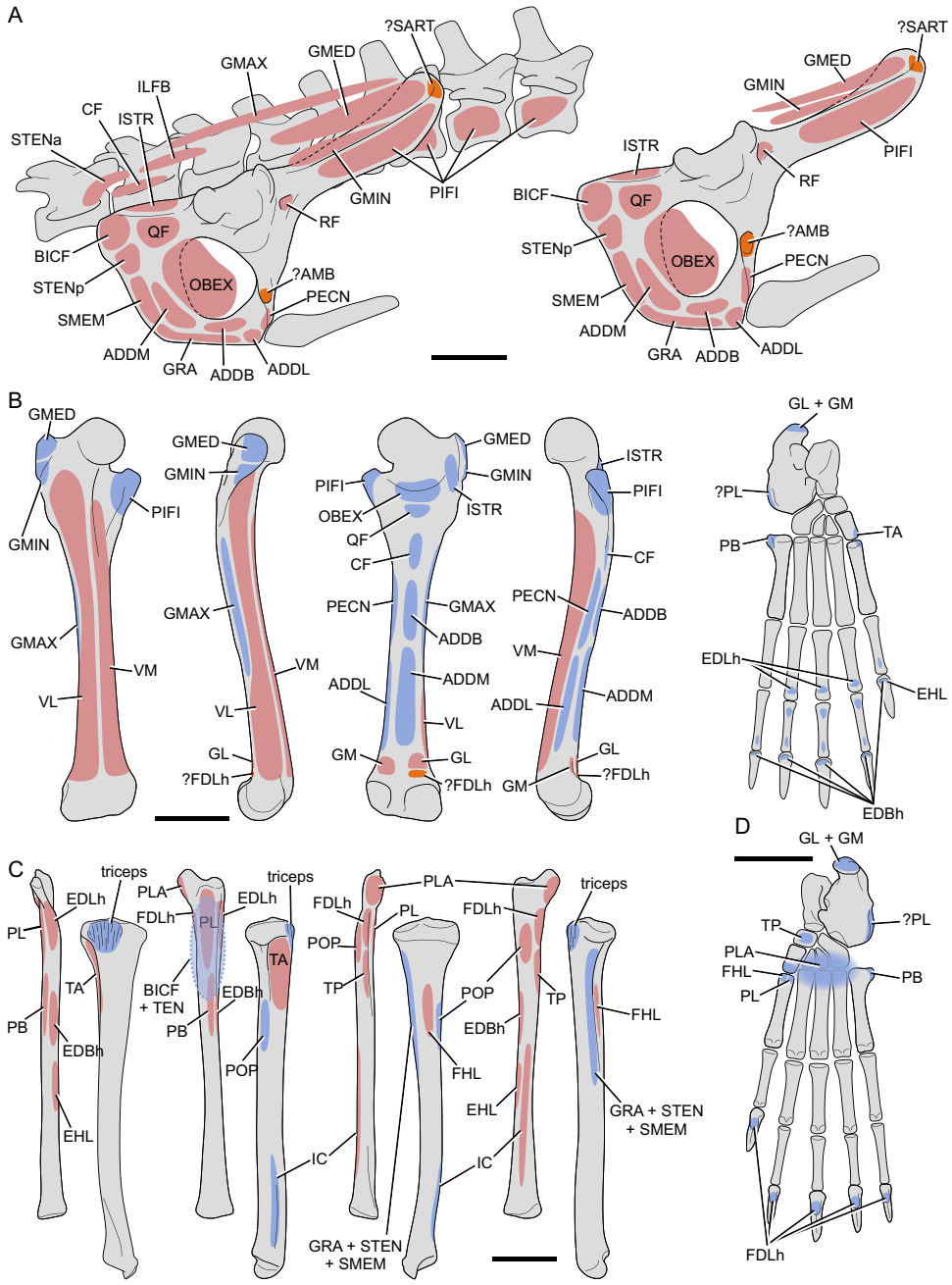

Figure 9. Reconstructed muscle attachments in *Vincelestes*. A, pelvis and axial skeleton, in lateral and ventrolateral views. B, femur in anterior, lateral, posterior, and medial views. C, tibia and fibula in anterior, lateral, posterior, and medial views. D, pes in dorsal (top) and ventral (bottom) views; distal tarsals and phalanges based on *Jeholodens*, *Zhangheotherium*, *Akidolestes*, and *Henkelotherium*. Red denotes inferred origins, blue denotes inferred insertions, and orange denotes ambiguous attachments (see text). Scale = 10 mm. See Table 8 for muscle abbreviations.

TABLE 8. RECONSTRUCTED ORIGINS AND INSERTIONS IN *VINCELESTES NEUQUENIANUS*. LOI, LEVEL OF INFERENCE IN THE SCHEME OF WITMER (1995).

		Origin		Insertion	
Muscle	Abbreviation	Attachment	LOI	Attachment	LOI
Iliotibialis	IT	Base of ilium, immediately anterior to acetabulum (rectus femoris [RF], pit); and sacral and proximalmost caudal vertebrae (gluteus maximus [GMAX])	II	Tuberosity on anteroproximal end of cnemial crest of tibia, via common "triceps" tendon (RF); lateral aspect of femoral shaft distal to GrTr (GMAX)	I/II′
Ambiens/sartorius	AMB/SART	Lateral aspect of pubis anteroventral to acetabulum, on or near pubic tubercle (AMB) *OR* from anterolateral apex of ilium (SART)	II′	Tuberosity on anteroproximal end of cnemial crest of tibia, via common "triceps" tendon	I
Vastus lateralis	VL	Lateral aspect of much of femoral shaft, distal to IF insertions	I′	Tuberosity on anteroproximal end of cnemial crest of tibia, via common "triceps" tendon	I
Vastus medialis	VM	Medial aspect of much of femoral shaft, distal and lateral to PIFI insertion	I′	Tuberosity on anteroproximal end of cnemial crest of tibia, via common "triceps" tendon	I
Iliofemoralis	IF	Shallow gluteal fossa occupying dorsal half of iliac blade (possibly extending posteriorly over last sacral or first caudal vertebra); via two heads (gluteus medius [GMED] and minimus [GMIN])	II	Anterolateral aspect of greater trochanter on lateral proximal femur	II
Iliopsoas	ILPS	Shallow iliac fossa occupying ventral half of iliac blade, extending onto sacral or posteriormost lumbar vertebrae; number of divisions uncertain	II	Anteromedial aspect of lesser trochanter on medial proximal femur	II
Puboischiofemoralis externus	PIFE	Much of lateral surface of pubis and ischium surrounding obturator foramen; via two heads, one anterior (obturator externus [OBEX]) and one posterior (quadratus femoris [QF])	II′	Posterior proximal femur in depression between greater and lesser trochanters	II′
Tenuissimus	TEN	Transverse processes of anterior caudal vertebrae, deep to posterior IT origin (no postacetabular ilium)	II	Lateral distal crural fascia, deep to BICF insertion	II′

Table 8. Continued.

Muscle	Abbreviation	Origin		Insertion	
		Attachment	LOI	Attachment	LOI
Flexor tibialis internus	FTI	Posterolateral ischium; via at least two heads (biceps femoris [BICF] and semimembranosus [SMEM]); dorsal head (BICF) originating near ischiadic tuberosity on posterodorsal apex	II	Posteromedial tibia, in association with GRA and STEN insertions (SMEM) and fascia of lateral crus (BICF)	II′
Semitendinosus	STEN	Via two heads: ventral/posterior head from lateral aspect of ischiadic tuberosity (STENp), dorsal/anterior head from transverse processes of sacral or anteriormost caudal vertebrae (STENa)	II′	Posteromedial tibia, in association with GRA and SMEM and BICF insertions	II′
Gracilis	GRA	Ventral pubis and ischium along puboischiadic symphysis	II′	Medial tibia, in association with (and superficial to) SMEM, BICF, and STEN	II′
Pectineus	PECN	Anterolateral aspect of pubis, on or near pubic tubercle and epipubis	I′	Medial to posteromedial aspect of femoral midshaft	I′
Adductor longus	ADDL	Anteroventral pubis, near epipubis	I′	Posteromedial aspect of distal femur	I′
Adductor femoris	ADD	Close to the puboischiadic suture on ventral pubis and ischium; via two heads (adductor magnus [ADDM] and adductor brevis [ADDB])	II′	Posterior aspect of femoral shaft	II′
Ischiotrochantericus	ISTR	Dorsal ischium (longitudinal depression facing dorsolaterally), plus medial surface of ischium	II	Posterior aspect of greater trochanter	II′
Caudofemoralis	CF	Transverse processes of proximal caudal vertebrae, deep to STENa origin; via single head	II′	Posterior aspect of femoral shaft, distal to OBEX and QF insertions	II′
Gastrocnemius lateralis	GL	Posterolateral distal femur, proximal to lateral condyle	I′	Apex of calcaneal tuber	II
Gastrocnemius medialis	GM	Posteromedial distal femur, proximal to medial condyle	II′	In common with GL	II
Plantaris	PLA	Posterior aspect of proximal fibula (parafibular process remains unknown)	II′	Plantar fascia on ventral aspect of pes, possibly continuing on to tarsals or metatarsals	II′

TABLE 8. CONTINUED.

		Origin		Insertion	
Muscle	Abbreviation	Attachment	LOI	Attachment	LOI
Flexor digitorum longus (hindlimb)	FDLh	Posteromedial aspect of proximal fibula	II′	Tendon that runs to insert on flexor tubercles of unguals	II
Flexor digitorum brevis	FDB	Dorsal (deep) surface of plantar fascia and adjacent tarsals and metatarsals	II′	Plantar aspect of proximal phalanges	II′
Flexor hallucis longus	FHL	Posterior aspect of proximal tibia; may have been absent	II′	Plantar aspect of entocuneiform and metatarsal I base, possibly also including plantar fascia; may have been absent	II′
Extensor digitorum longus (hindlimb)	EDLh	Anterior aspect of proximal fibula	II′	Dorsal aspect of distal phalanges II–IV	II′
Extensor digitorum brevis (hindlimb)	EDBh	Anterior aspect of proximal fibula, distal to EDLh origin; number of heads uncertain	II′	Dorsal aspect of penultimate phalanges and extensor processes of unguals	I
Extensor hallucis longus	EHL	Anteromedial aspect of midshaft of fibula	II′	Extensor process on dorsal aspect of digit I ungual	II
Tibialis anterior	TA	Anterolateral aspect of proximal tibia, in lateral fossa of cnemial crest	II	Dorsomedial proximal aspect of entocuneiform or metatarsal I	II′
Peroneus longus	PL	Lateral proximal fibula, in large fossa	II′	Ventral aspect of base of metatarsal I, possibly via the distolateral shelf (peroneal shelf) of calcaneum	II′
Peroneus brevis	PB	Anterolateral proximal fibula, anterior to PL origin	II′	Base of metatarsal V, on laterally projecting process	II′
Tibialis posterior	TP	Posteromedial aspect of proximal fibular shaft, distal to expanded head	II′	Plantar aspect of navicular	II′
Popliteus	POP	Posteromedial aspect of fibular head, proximal to PP origin	II	Posterolateral proximal tibia	II′
Interosseus cruris	IC	Medial aspect of distal fibular shaft	II′	Lateral aspect of distal tibial shaft	II′

8. As noted above, *Vincelestes* was added as its own novel operational taxonomic unit to the data set of Bishop and Pierce (2024b); reconstructed states at the node Cladotheria (Table S8) were used to clarify remaining uncertainties. Some character states remained ambiguous for this node, and these were resolved for *Vincelestes* as follows.

Character 1. Without any positive evidence for a splitting of the ITp into separate heads (i.e., GMAX and FCOC), only a single head is inferred here (state 0, level II′ inference).

Character 5. Unlike many other Mesozoic crown mammals, *Vincelestes* lacks any indication of a third trochanter or other crest on the lateral femoral shaft (state 3, level II′ inference).

Character 6. The origin of the AMB is presently unable to be resolved, and hence

it is unclear whether the muscle originated more ventrally, in the plesiomorphic configuration (i.e., AMB-like), or more dorsally from the ilium, in the therian configuration (i.e., SART-like). In the absence of osteological evidence, it is currently not possible to discriminate between the two states.

Character 11. Although optimization here reconstructs the patella as ancestrally present for cladotherians, previous work has suggested that ossified patellae evolved independently in marsupials and placentals (Samuels et al., 2017). A patella has not yet been identified in *Vincelestes*, although this may well be due to the disarticulated nature of most of the available material. A patella is not present in the closely related cladotherian *Henkelotherium guimarotae*, which is represented by articulated material (Jäger et al., 2019).

Character 12. Assuming that a twofold subdivision of the IF mass was a precursor to a threefold subdivision on the line to therians, this precludes state 0. Without any positive evidence either way, only two gluteal heads are reconstructed here in *Vincelestes* (state 1, level II′ inference). This captures the two main heads that are consistently present in extant mammals; other heads such as the pyriformis are much smaller and tend to be positioned closer to the hip joint, thus having relatively low functional significance.

Character 15. Without any positive evidence for a splitting of the muscle mass, the PIFI is conservatively reconstructed as singular here (state 0, level II′ inference; an "iliopsoas").

Character 22. Parsimony recovers the ILFB as absent for Cladotheria, which is incongruous with the reconstruction for character 21 and its presence in some therians. An indirect, soft-tissue attachment to the lateral crural fascia is inferred here (state 2, level III′ inference), which is the condition observed in therians when the muscle is present.

Character 36. The puboischiadic plate of *Vincelestes* is notably large in relation to the ilium, compared to that typically observed in therians, and this would provide ample room for the origin of two separate adductor masses. Both short (ADDB) and large (ADDM) heads are reconstructed here (state 1, level II′ inference).

Character 39. As discussed by Bishop and Pierce (2024b), it is not currently possible to discern whether the single-headed condition in monotremes is plesiomorphic or apomorphic. A single head is conservatively assumed here (state 0, level II′ inference), although in functional terms, the presence of a second head (i.e., the GEM) would be relatively small and subsidiary to the larger muscle belly (i.e., the OBIN).

Character 43. Vincelestes possesses a very sizeable tail for a mammal (≫30 caudal vertebrae; Rougier, 1993), and its proximal caudal vertebrae bear well-developed transverse processes. An origin similar to that observed in monotremes is tentatively assumed here, in which the CF retains an osseous contact (state 2, level II′ inference).

Character 46. The gastrocnemii are ubiquitous among amniotes, and so the GE can be confidently inferred as present in *Vincelestes*. The development of an incipient parafibula in more basal mammals is taken to indicate the differentiation of the PLA prior to the origin of Cladotheria, but the SOL is assumed to be an apomorphy of Theria; state 2 is reconstructed here (level II′ inference).

Character 48. Irrespective of state 1 or 2, the locus of attachment is somewhere around the proximal fibula. It is unclear the extent to which *Vincelestes* possessed a parafibula, although the morphology of the structure preserved at the proximal end in MACN-N 38 is comparable to the structure observed in other taxa with such a process (e.g., *Megazostrodon*, basal therians), and so state 1 is tentatively inferred (level II′ inference).

Character 49. As per character 46, the SOL is presumed to be absent in *Vincelestes* (state 0, level II′ inference).

Character 52. As per character 48, the PLA is inferred to be present in *Vincelestes*, although the exact manner of the insertion of this muscle, distal to the plantar fascia, is not certain (states 1/2, level II′ inference).

Character 53. As per character 46, the SOL is presumed to be absent in *Vincelestes* (state 0, level II′ inference).

Character 55. The locus of the FDLh origin in amniotes is generally centered around the posterior proximal fibula, and this area is conservatively interpreted as the primary attachment for the FDLh in *Vincelestes*. In lieu of definitive evidence of a parafibula in *Vincelestes*, the origin is reconstructed as from the posterior aspect of the fibular head (state 3, level II′ inference).

Character 59. It is unclear if the FHL of therians is homologous with the FHL observed in crocodylians and *Sphenodon*, and indeed the "therian FHL" may be a therian apomorphy. If it was present in *Vincelestes*, it would have presumably taken origin from the posteroproximal tibia (state 2).

Character 60. Following the same reasoning as the previous character, if a FHL were present in *Vincelestes*, it would have presumably inserted in a therian-like fashion (state 2).

Character 61. The locus of the EDLh origin in amniotes is generally centered around the anterior knee region, with mammals typically involving more of the fibula or tibia than the femur. Given the modifications to the fibula prior to Mammaliaformes (i.e., spatulate shape, incipient parafibula), this suggests significant reorganization of the associated soft tissues as well, and the origin is tentatively reconstructed here as from the anterior aspect of the fibular head (state ~2, level II′ inference).

Character 63. It remains uncertain as to when any "extra peroneal heads" differentiated on the line to therians, and hence it is currently ambiguous whether the EDBh was accompanied by other bellies in *Vincelestes*.

Character 66. The EHL is ubiquitous among amniotes and can be confidently inferred as present in *Vincelestes*. Its locus of origin is centered around the anterior fibula, and in the absence of any positive evidence, a middle-of-the-road approach is taken and the origin reconstructed at the fibular midshaft (state 2, level II′ inference). Extension of the origin onto the parafibula or medial tibia is apomorphic for one genus of monotreme or another, and so it is not considered here to be phylogenetically informative.

Character 71. The PL can unambiguously be inferred to have originated from around the lateral knee region, but specifically where cannot be discerned. The more mammalian construction of the bones (especially the lightly constructed fibula) around the knee joint in *Vincelestes* supports a more mammalian manifestation of muscle attachment being present. The origin is here reconstructed as from the lateral proximal fibula (state 3, level II′ inference), where a large fossa provides ample area for attachment.

Character 73. The calcaneum of *Vincelestes* possesses a well-developed lateral corner to the peroneal shelf and a well-formed tuber, which are elsewhere inferred as probable osteological indicators of states 1 and 3, respectively. However, as a crown mammal, it is likely to have possessed an insertion more on the ventral aspect of the medial pes (Bishop and Pierce, 2024b). As such, although the PL may have gained attachment to the peroneal shelf, a terminal insertion on the plantar aspect of metatarsal 1 is inferred here (state 4, level II′ inference).

Character 74. The existence of two peroneal heads is supported here (character 70), with the PB inserting in a mammal-like fashion somewhere along pedal ray V. *Vincelestes* possesses a pronounced lateral projection on the base of metatarsal V (Rougier, 1993), and

the PB is inferred to have inserted on this process (state 4, level II′ inference).

Character 75. The exact origin of the PP in *Vincelestes* is uncertain, but the locus is inferred to be the posterior aspect of the crus, deep to the FDLh but superficial to the POP.

Character 77. The origin for the POP in *Vincelestes* is uncertain, although the general locus of attachment is around the proximal fibula, and this is conservatively reconstructed as the principal site of origin (∼state 0, level II′ inference), with limited, if any, attachment to the femur.

DISCUSSION

Comparison to Prior Studies

The reconstructions presented here offer a new, more comprehensive account of hindlimb muscular anatomy across key stages of (pretherian) synapsid evolution. For some of the focal taxa considered here, this represents the first extensive interpretation of the fossil evidence, whereas in other taxa, it represents a revised update upon older works (Romer, 1922; Colbert, 1948; Kemp, 1978; DeFauw, 1986). Short of a muscle-by-muscle, study-by-study comparison to the interpretations of previous authors, some of which were already noted above, a few overarching points may be made here to provide a broader context for evaluating the merit of the present reconstructions.

There are numerous points of minor difference in comparison to prior studies, but the reconstructions provided here are nonetheless broadly consilient with previous interpretations of the general locus of attachment of most hip muscles. More importantly, however, the present study provides the first detailed interpretation of all muscles crossing the knee and ankle joints, in addition to those crossing the hip. It therefore offers an important basis for interpreting crural and pedal anatomy in fossil taxa. Whereas many prior studies have interpreted fossil hindlimb osteology with respect to musculature, the majority of such interpretations were restricted to hip muscles (e.g., Parrington, 1961; Boonstra, 1964; Jenkins, 1971; Jenkins and Parrington, 1976; Kemp, 1978, 1980a,b; King, 1981, 1985; Sullivan et al., 2013; Guignard et al., 2018, 2019). This is probably due, in no small part, to the anatomical focus of the seminal works of Gregory and Camp (1918) and Romer (1922), the latter of which serving as the *sine qua non* point of reference for almost all subsequent studies over the following 100 years. Even then, subsequent studies often did not reconstruct every hip muscle, instead tending to focus on those of greater evolutionary significance, especially the IF, PIFI, PIFE, and CF, i.e., those which underwent major reorganization on the line to mammals. Several studies have also briefly considered biarticular hip muscles that crossed the knee, those comprising the triceps femoris and crural flexor ("hamstring") groups, but rarely have these muscles' crural insertions been given the same level of attention as their pelvic origins (Gregory and Camp, 1918; Romer, 1922; Colbert, 1948; DeFauw, 1986; Ray and Chinsamy, 2003; Ray, 2006). Only Walter (1988) provided any detailed interpretation of muscles originating distal to the knee.

Reconstructing only a subset of the full complement of limb muscles can only ever offer an incomplete picture of anatomy in a given extinct species and its evolution through time. More critically, attempting to do so runs the risk of failing to account for the attachments of other muscles that are not considered, yet which "competed" for attachment space on the available bony surfaces. Thus, prior studies have at times interpreted the IF as originating from the entire iliac blade, affording insufficient space for the ILFB or IT, or they have reconstructed the PIFE as originating from the entire ischium, affording insufficient space for the ADD, FTI, or PIT (e.g., Kemp, 1980a,b; King, 1981; Guignard

et al., 2018). The simplistic and erroneous reconstructions that result can hinder assessments of muscle functional evolution, especially if the unreconstructed muscles were an important functional complement (as agonist or antagonist) to the muscles that were reconstructed.

One additional point worth noting is that hypotheses of limb muscle homology across tetrapods have changed considerably over the past 100 years, stemming from advances in anatomical and embryological comparative data sets (see Diogo and Molnar, 2014; Diogo et al., 2016). Several points of difference between the present set of reconstructions and those of certain prior studies may be attributed to the use of now-outdated homology schemes by prior studies. For example, King (1985) and DeFauw (1986) reconstructed the ILFB as originating from the ischium in various dicynodonts, assuming homology of this muscle and the mammalian BICF. The ILFB and BICF are now understood to be nonhomologous, and as such, the former is consistently reconstructed here as originating dorsally from or near the posterior ilium, and the latter (or its homologue, the FTI2) is consistently reconstructed as originating ventrally from the posterior ischium. Consideration of this issue is essential to undertaking an even-handed appraisal of historical interpretations, especially if these are to form the basis for new investigations.

Uncertainty in Reconstructions

While the present set of reconstructions is more comprehensive than prior attempts, and the current reconstructions are based on the largest data set for extinct and extant anatomy thus far assembled (Bishop and Pierce, 2024b), they are not infallible. Various aspects come with a level of uncertainty, resulting from ambiguity in the interpretation of available evidence, and they may be subject to re-evaluation in light of new fossil or developmental data. Many interpretations are only modestly supported, qualifying as level II′ inferences in the credibility scheme of Witmer (1995). Contrasting reconstructions may have important consequences for higher-level functional interpretations such as locomotor performance and behavior.

In addition to a given muscle's presence or absence, and the general locus of its origins and insertions with respect to the underlying skeleton, the muscle maps presented here also outline interpreted areas of attachment for individual muscles. Given the paucity of direct osteological evidence for precisely delimiting attachment area in most muscles (especially those with fleshy attachments), reconstructing these areas remains a subjective process and therefore carries a higher level of uncertainty compared to other aspects of a reconstruction (e.g., presence or absence). Such uncertainty is likely to be more prevalent in extinct taxa that are more phylogenetically distant or morphologically disparate from their nearest extant relatives. As noted by Bryant and Seymour (1990), error in reconstructed muscle attachment areas may lead to error in estimates of muscle size or strength (i.e., force-generating capacity). However, even in extant species where attachment areas have been quantitatively measured, the correlation between attachment area and muscle strength can be of variable quality and can vary considerably across the specific muscles and taxa considered (Fahn-Lai et al., 2020; Bates et al., 2021; Cuff et al., 2023). Errors in estimated muscle attachment area may therefore be secondary to other sources of error or variation in their possible consequences for downstream analyses. Furthermore, growing numbers of studies have developed alternative approaches to estimating muscle strength in extinct species, which do not require quantitative data on attachment areas, yet which remain grounded in empirical data sets derived from extant taxa (e.g., Sellers et al., 2013; Bates and Falkingham,

2018; Bishop et al., 2021a,b). Thus, imprecision in reconstructed muscle attachment areas may not actually matter in some situations.

Beyond estimation of muscle strength, reconstructions of attachment areas can potentially influence functional analyses by determining the spatial distribution of muscular forces in a biomechanical model. The centroid of a given attachment area is frequently used to guide the creation of muscle lines of action in musculoskeletal (rigid body) models and may therefore influence a muscle's length or its moment arm(s) with respect to joint angle (Brassey et al., 2017; Bishop et al., 2018, 2021a; Brocklehurst et al., 2022). Muscle attachment areas, or their centroids, also dictate how muscle forces are applied to bony structures in finite element models (Sellers et al., 2017; Bishop et al., 2018; Cost et al., 2020). The extent to which error in reconstructed attachment areas may significantly affect downstream analyses and interpretations in these contexts is seldom investigated (Brassey et al., 2017), although it might be expected that approaches based on area centroids should be less sensitive than those that are not, since centroids will be more robust to finer-scale variation in attachment boundaries. Considering the great diversity in musculoskeletal anatomy and function encountered in Synapsida (let alone broader taxonomic groups), and the diversity of approaches used to study musculoskeletal function, it is difficult to draw overarching generalizations about how uncertainty in muscle attachment reconstruction may affect higher-level inferences. To that end, future studies that draw upon the present set of reconstructions should carefully consider the aspects (if any) of uncertainty that are most critical to the question at hand and conduct appropriate sensitivity analyses to evaluate the consequences of alternative reconstructions (Bishop et al., 2021a).

CONCLUSION

Phylogenetically informed reconstructions of hindlimb musculature have been presented for eight exemplar fossil synapsid taxa that collectively document much of the anatomical transformation that occurred on the line to therian mammals. In the future, a similar set of reconstructions for exemplar taxa will be produced for the forelimb musculature. Such reconstructions provide an improved foundation for functional analysis of the appendicular skeleton, although detailed focus on pedal function distal to the ankle will first require additional efforts to understand the intrinsic soft tissue anatomy not considered here.

ACKNOWLEDGMENTS

Special thanks are due to the museum curatorial and collections staff for access to specimens in their care: C. Mehling and A. Gishlick (AMNH), S. Jirah, B. Rubidge, and B. Zipfel (BP), O. Rauhut (BSPG), N. Mchunu (CGS), K. Angielczyk, W. Simpson, and A. Stroup (FMNH), I. Werneburg and A. Krahl (GPIT), A. Martinelli, J. Escobar, and M. Ezcurra (MACN), C. Byrd, E. Biedron, M. Omura, S. Johnston, C. Green, and A. Kowalczyk (MCZ), M. Day (NHMUK), E. Butler and J. Botha (NMQR), P. Ortiz and R. González (PVL), Z. Skosan and C. Browning (SAM), H. Fourie (TM), M. Lowe and R. Stebbings (UMZC), and H. Sues, A. Millhouse, and R. Masters (USNM). Helpful discussion and feedback from many colleagues, including C. Kammerer, B. Stuart, M. Wright, R. Brocklehurst, and the aforementioned museum staff, are also greatly appreciated. Lastly, A. Biewener is thanked for handling the manuscript, and two anonymous reviewers are thanked for suggestions on a prior version of the manuscript. This work was financially supported by the U.S. National Science Foundation, grants DEB-1754459 and

EAR-2122115, and the William F. Milton Fund, Harvard University.

LITERATURE CITED

Bates, K. T., and P. L. Falkingham. 2018. The importance of muscle architecture in biomechanical reconstructions of extinct animals: a case study using *Tyrannosaurus rex*. *Journal of Anatomy* 233: 625–635.

Bates, K. T., L. Wang, M. Dempsey, S. Broyde, M. J. Fagan, and P. G. Cox. 2021. Back to the bones: do muscle area assessment techniques predict functional evolution across a macroevolutionary radiation? *Journal of the Royal Society Interface* 18: 20210324.

Bendel, E.-M., C. F. Kammerer, R. M. H. Smith, and J. Fröbisch. 2023. The postcranial anatomy of *Gorgonops torvus* (Synapsida, Gorgonopsia) from the late Permian of South Africa. *PeerJ* 11: e15378.

Bishop, P. J., A. R. Cuff, and J. R. Hutchinson. 2021a. How to build a dinosaur: musculoskeletal modelling and simulation of locomotor biomechanics in extinct animals. *Paleobiology* 47: 1–38.

Bishop, P. J., S. A. Hocknull, C. J. Clemente, J. R. Hutchinson, R. S. Barrett, and D. G. Lloyd. 2018. Cancellous bone architecture and theropod dinosaur locomotion. Part II—a new approach to reconstructing posture and locomotor biomechanics in extinct tetrapod vertebrates. *PeerJ* 6: e5779.

Bishop, P. J., and S. E. Pierce. 2024a. The fossil record of appendicular muscle evolution in Synapsida on the line to mammals. Part I—forelimb. *The Anatomical Record* 307: 1764–1825.

Bishop, P. J., and S. E. Pierce. 2024b. The fossil record of appendicular muscle evolution in Synapsida on the line to mammals. Part II—hindlimb. *The Anatomical Record* 307: 1826–1896.

Bishop, P. J., M. A. Wright, and S. E. Pierce. 2021b. Whole-limb scaling of muscle mass and force-generating capacity in amniotes. *PeerJ* 9: e12574.

Blob, R. W. 2001. Evolution of hindlimb posture in nonmammalian therapsids: biomechanical tests of paleontological hypotheses. *Paleobiology* 27: 14–38.

Bonaparte, J. F. 1963. Descripción del esqueleto postcraneano de Exaeretodon (Cynodontia – Traversodontidae). *Acta Geológica Lilloana* 4: 5–52.

Boonstra, L. D. 1934. A contribution to the morphology of the Gorgonopsia. *Annals of the South African Museum* 31: 137–174.

Boonstra, L. D. 1964. The girdles and limbs of the pristerognathid Therocephalia. *Annals of the South African Museum* 48: 121–165.

Botha, J., and K. D. Angielczyk. 2007. An integrative approach to distinguishing the late Permian dicynodont species *Oudenodon bainii* and *Tropidostoma microtrema* (Therapsida: Anomodontia). *Palaeontology* 50: 1175–1209.

Brassey, C. A., S. C. R. Maidment, and P. M. Barrett. 2017. Muscle moment arm analyses applied to vertebrate paleontology: a case study using *Stegosaurus stenops* Marsh, 1887. *Journal of Vertebrate Paleontology* 37: e1361432.

Brinkman, D. 1981. The structure and relationships of the dromasaurs (Reptilia: Therapsida). *Breviora* 465: 1–34.

Brocklehurst, R. J., P. Fahn-Lai, S. Regnault, and S. E. Pierce. 2022. Musculoskeletal modeling of sprawling and parasagittal forelimbs provides insight into synapsid postural transition. *iScience* 25: 103578.

Broili, F., and J. Schröder. 1935. Über die Skelettrests einers Gorgonopsiers aus den unteren Beaufort-Schichten. *Sitzungsberichte der mathematisch-naturwissenchaftlichen Abteilung der Baierischen Akademie der Wissenschaften zu München* 1935: 279–330.

Bryant, H. N., and K. L. Seymour. 1990. Observations and comments on the reliability of muscle reconstruction in fossil vertebrates. *Journal of Morphology* 206: 109–117.

Burch, S. H. 2014. Complete forelimb myology of the basal theropod dinosaur *Tawa hallae* based on a novel robust muscle reconstruction method. *Journal of Anatomy* 225: 271–297.

Carrano, M. T., and J. R. Hutchinson. 2002. Pelvic and hindlimb musculature of *Tyrannosaurus rex* (Dinosauria: Theropoda). *Journal of Morphology* 253: 207–228.

Chen, M., and Z.-X. Luo. 2013. Postcranial skeleton of the Cretaceous mammal *Akidolestes cifellii* and its locomotor adaptations. *Journal of Mammalian Evolution* 20: 159–189.

Colbert, E. H. 1948. The mammal-like reptile *Lycaenops*. *Bulletin of the American Museum of Natural History* 89: 353–404.

Cost, I. N., K. M. Middleton, K. C. Sellers, M. S. Echols, L. M. Witmer, J. L. Davis, and C. M. Holliday. 2020. Palatal Biomechanics and its Significance for Cranial Kinesis in *Tyrannosaurus rex*. *The Anatomical Record* 303: 999–1017.

Cuff, A. R., A. L. A. Wiseman, P. J. Bishop, K. B. Michel, R. Gaignet, and J. R. Hutchinson. 2023. Anatomically grounded estimation of hindlimb muscle sizes in Archosauria. *Journal of Anatomy* 242: 289–311.

DeFauw, S. L. 1986. *The Appendicular Skeleton of African Dicynodonts*. Ph.D. thesis. Detroit (MI): Wayne State University.

De Oliveira, T. V., M. B. Soares, and C. L. Schultz. 2010. *Trucidocynodon riograndensis* gen. nov. et sp. nov. (Eucynodontia), a new cynodont from the Brazilian Upper Triassic (Santa Maria Formation). *Zootaxa* 2382: 1–71.

Diogo, R., G. Bello-Hellegouarch, T. Kohlsdorf, B. Esteve-Altava, and J. Molnar. 2016. Comparative myology and evolution of marsupials and other vertebrates, with notes on complexity, bauplan and "scala naturae." *The Anatomical Record* 299: 1224–1255.

Diogo, R., and J. Molnar. 2014. Comparative anatomy, evolution, and homologies of tetrapod hindlimb muscles, comparison with forelimb muscles, and deconstruction of the forelimb–hindlimb serial homology hypothesis. *The Anatomical Record* 297: 1047–1075.

Fahn-Lai, P., A. A. Biewener, and S. E. Pierce. 2020. Broad similarities in shoulder muscle architecture and organization across two amniotes: implications for reconstructing non-mammalian synapsids. *PeerJ* 8: 8556.

Fernandez, V., F. Abdala, K. J. Carlson, D. C. Cook, B. S. Rubidge, A. M. Yates, and P. Tafforeau. 2013. Synchrotron reveals Early Triassic odd couple: injured amphibian and aestivating therapsid share burrow. *PLOS One* 8: e64978.

Fourie, H., and B. S. Rubidge. 2007. The postcranial skeletal anatomy of the therocephalian *Regisaurus* (Therapsida: Regisauridae) and its utilization for biostratigraphic correlation. *Palaeontologia africana* 42: 1–16.

Gambaryan, P. P., A. A. Aristov, J. M. Dixon, and G. Y. Zubtsova. 2002. Peculiarities of the hind limb musculature in monotremes: an anatomical description and functional approach. *Russian Journal of Theriology* 1: 1–36.

Gregory, W. K., and C. L. Camp. 1918. Studies in comparative myology and osteology. *Bulletin of the American Museum of Natural History* 38: 447–563.

Guignard, M. L., A. G. Martinelli, and M. B. Soares. 2018. Reassessment of the postcranial anatomy of *Prozostrodon brasiliensis* and implications for postural evolution of non-mamaliaform cynodonts. *Journal of Vertebrate Paleontology* 38: e1511570.

Guignard, M. L., A. G. Martinelli, and M. B. Soares. 2019. The postcranial anatomy of *Brasilodon quadrangularis* and the acquisition of mammaliaform traits among non-mammaliaform cynodonts. *PLOS One* 14: e0216672.

Haughton, S. H. 1929. On some new therapsid genera. *Annals of the South African Museum* 28: 55–78.

Hutchinson, J. R. 2001a. The evolution of femoral osteology and soft tissues on the line to extant birds (Neornithes). *Zoological Journal of the Linnean Society* 131: 169–197.

Hutchinson, J. R. 2001b. The evolution of pelvic osteology and soft tissues on the line to extant birds (Neornithes). *Zoological Journal of the Linnean Society* 131: 123–168.

Hutchinson, J. R. and M. Garcia. 2002. *Tyrannosaurus* was not a fast runner. *Nature* 415: 1018–1021.

Jäger, K. R. K., Z.-X. Luo, and T. Martin. 2019. Postcranial skeleton of *Henkelotherium guimarotae* (Cladotheria, Mammalia) and locomotor adaptation. *Journal of Mammalian Evolution* 27: 349–372.

Jenkins, F. A., Jr. 1970. The Chañares (Argentina) Triassic reptile fauna VII. The postcranial skeleton of the traversodontid *Massetognathus pascuali* (Therapsida, Cynodontia). *Breviora* 352: 1–28.

Jenkins, F. A., Jr. 1971. The postcranial skeleton of African cynodonts. *Bulletin of the Peabody Museum of Natural History* 36: 1–216.

Jenkins, F. A., Jr., and F. R. Parrington. 1976. The postcranial skeletons of the Triassic mammals *Eozostrodon*, *Megazostrodon* and *Erythrotherium*. *Philosophical Transactions of the Royal Society of London, Series B* 273: 387–431.

Ji, Q., Z. Luo, and S.-a. Ji. 1999. A Chinese triconodont mammal and mosaic evolution of the mammalian skeleton. *Nature* 398: 326–330.

Kemp, T. S. 1978. Stance and gait in the hindlimb of a therocephalian mammal-like reptile. *Journal of Zoology* 186: 143–161.

Kemp, T. S. 1980a. Aspects of the structure and functional anatomy of the Middle Triassic cynodont *Luangwa*. *Journal of Zoology* 191: 193–239.

Kemp, T. S. 1980b. The primitive cynodont *Procynosuchus*: structure, function and evolution of the postcranial skeleton. *Philosophical Transactions of the Royal Society of London, Series B* 288: 217–258.

Kemp, T. S. 1982. *Mammal-like Reptiles and the Origin of Mammals*. London: Academic Press.

Kemp, T. S. 1986. The skeleton of a baurioid therocephalian therapsid from the Lower Triassic (*Lystrosaurus* Zone) of South Africa. *Journal of Vertebrate Paleontology* 6: 215–232.

Kemp, T. S. 2005. *The Origin and Evolution of Mammals*. Oxford: Oxford University Press.

Kemp, T. S. 2006. The origin and early radiation of the therapsid mammal-like reptiles: a palaeobiological hypothesis. *Journal of Evolutionary Biology* 19: 1231–1247.

Kemp, T. S. 2016. *The Origin of Higher Taxa*. Oxford: Oxford University Press.

King, G. M. 1981. The functional anatomy of a Permian dicynodont. *Philosophical Transactions of the Royal Society of London, Series B* 291: 243–322.

King, G. M. 1985. The postcranial skeleton of *Kingoria nowacki* (von Huene) (Therapsida: Dicynodontia). *Zoological Journal of the Linnean Society* 84: 263–289.

King, G. M. 1990. *The Dicynodonts: A Study in Palaeobiology*. London: Chapman and Hall.

Krebs, B. 1991. Das Skelett von *Henkelotherium guimarotae* gen. et sp. nov. (Eupantotheria, Mammalia) aus dem Oberen Jura von Portugal. *Berliner Geowissenschaftliche Abhandlungen* A133: 1–110.

Lai, P. H., A. A. Biewener, and S. E. Pierce. 2018. Three-dimensional mobility and muscle attachments in the pectoral limb of the Triassic cynodont *Massetognathus pascuali* (Romer, 1967). *Journal of Anatomy* 232: 383–406.

Liu, J., V. P. Schneider, and P. E. Olsen. 2017. The postcranial skeleton of *Boreogomphodon* (Cynodontia: Traversodontidae) from the Upper Triassic of North Carolina, USA, and the comparison with other traversodontids. *PeerJ* 5: e3521.

Luo, Z.-X., and Q. Ji. 2005. New study on dental and skeletal features of the Cretaceous "symmetrodontan" mammal *Zhangheotherium*. *Journal of Mammalian Evolution* 12: 337–357.

Maddison, W. P., and D. R. Maddison. 2021. Mesquite: a modular system for evolutionary analysis. Version 3.61 [Internet]. [Cited 2021 June 2]. Available from: http://www.mesquiteproject.org.

Molnar, J. L., R. Diogo, J. R. Hutchinson, and S. E. Pierce. 2018. Reconstructing pectoral appendicular muscle anatomy in fossil fish and tetrapods over the fins-to-limbs transition. *Biological Reviews* 93: 1077–1107.

Molnar, J. L., R. Diogo, J. R. Hutchinson, and S. E. Pierce. 2020. Evolution of hindlimb muscle anatomy across the tetrapod water-to-land transition, including comparisons with forelimb anatomy. *The Anatomical Record* 303: 218–234.

Parrington, F. R. 1961. The evolution of the mammalian femur. *Proceedings of the Zoological Society of London* 137: 285–298.

Pusch, L.C., C. F. Kammerer, and J. Fröbisch. 2024. The origin and evolution of Cynodontia (Synapsida, Therapsida): reassessment of the phylogeny and systematics of the earliest members of this clade using 3D-imaging technologies. *The Anatomical Record* 307: 1634–1730.

Ray, S. 2006. Functional and evolutionary aspects of the postcranial anatomy of dicynodonts (Synapsida, Therapsida). *Palaeontology* 49: 1263–1286.

Ray, S, and A. Chinsamy. 2003. Functional aspects of the postcranial anatomy of the Permian dicynodont *Diictodon* and their ecological implications. *Palaeontology* 46: 151–183.

Reisz, R. R. 1986. Pelycosauria. *Handbuch der Paläoherpetologie* 17A: 1–100.

Romer, A. S. 1922. The locomotor apparatus of certain primitive and mammal-like reptiles. *Bulletin of the American Museum of Natural History* 46: 517–606.

Romer, A. S., and L. W. Price. 1940. *Review of the Pelycosauria*. Special Paper 28. Boulder (CO): Geological Society of America.

Rougier, G. W. 1993. *Vincelestes neuquenianus Bonaparte (Mammalia, Theria) un primitivo mamifero del Cretacio Inferior de la Cuenca Neuquina.* Ph. D. dissertation. Buenos Aires: Universidad Nacional de Buenos Aires.

Samuels, M. E., S. Regnault, and J. R. Hutchinson. 2017. Evolution of the patellar sesamoid bone in mammals. *PeerJ* 5: e3103.

Schaeffer, B. 1941. The pes of *Bauria cynops* Broom. *American Museum Novitates* 1103: 1–7.

Sellers, K. C., K. M. Middleton, J. L. Davis, and C. M. Holliday. 2017. Ontogeny of bite force in a validated biomechanical model of the American alligator. *Journal of Experimental Biology* 220: 2036–2046.

Sellers, W. I., L. Margetts, R. A. Coria, and P. L. Manning. 2013. March of the Titans: the locomotor capabilities of sauropod dinosaurs. *PLOS One* 8: e78733.

Sidor, C. A. 2022. New information on gorgonopsian pedal morphology based on articulated material from Zambia. *Journal of African Earth Sciences* 191: 104533.

Sullivan, C., J. Liu, E. M. Roberts, T. D. Huang, C. Yang, and S. Zhong. 2013. Pelvic morphology of a tritylodontid (Synapsida: Eucynodontia) from the Lower Jurassic of China, and some functional and phylogenetic implications. *Comptes Rendus Palevol* 12: 505–518.

Tatarinov, L. P. 2004. A postcranial skeleton of the gorgonopian *Viatkogorgon ivachnenkoi* (Reptilia, Theriodontia) from the Upper Permian Kotelnich locality, Kirov region. *Paleontological Journal* 38: 437–447.

von Huene, F. 1950. Die Theriodontier des ostafrikanischen Ruhuhu-Gebietes in der Tübinger Sammlung. *Neus Jahrbuch für Geologie und Palaontologie* 92: 47–136.

Walter, L. R. 1988. The limb posture of kannemeyeriid dicynodonts: functional and ecological considerations, PP. 89–97 IN: K. Padian, editor. *The Beginning of the Age of Dinosaurs*. Cambridge: Cambridge University Press.

Watson, D. M. S. 1917. The evolution of the tetrapod shoulder girdle and fore-limb. *Journal of Anatomy* 52: 1–63.

Watson, D. M. S. 1960. The Anomodont skeleton. *Transactions of the Zoological Society of London* 29: 131–209.

Witmer, L. M. 1995. The extant phylogenetic bracket and the importance of reconstructing soft tissues in fossils, PP. 19–33 IN: J. J. Thomason, editor. *Functional Morphology in Vertebrate Paleontology*. Cambridge: Cambridge University Press.

Photo on the front cover:

MCZ VPRA-1365 *Dimetrodon milleri*, an early synapsid from the Permian of Texas. Mounted skeleton on display in the Harvard Museum of Natural History. Photo by Christina Byrd.

US ISSN 0027-4100

MCZ Publications
Museum of Comparative Zoology
Harvard University
26 Oxford Street
Cambridge, MA 02138

mczpublications@mcz.harvard.edu